Spatio-Temporal Statistics with R

CHRISTOPHER K. WIKLE
ANDREW ZAMMIT-MANGION
NOEL CRESSIE

Chapman & Hall/CRC

Contents

Preface

We live in a complex world, and clever people are continually coming up with new ways to observe and record increasingly large parts of it so we can comprehend it better (warts and all!). We are squarely in the midst of a "big data" era, and it seems that every day new methodologies and algorithms emerge that are designed to deal with the ever-increasing size of these data streams.

It so happens that the "big data" available to us are often *spatio-temporal data*. That is, they can be indexed by spatial locations and time stamps. The space might be geographic space, or socio-economic space, or more generally network space, and the time scales might range from microseconds to millennia. Although scientists have long been interested in spatio-temporal data (e.g., Kepler's studies based on planetary observations several centuries ago), it is only relatively recently that statisticians have taken a keen interest in the topic. At the risk of two of us being found guilty of self-promotion, we believe that the book *Statistics for Spatio-Temporal Data* by Cressie and Wikle (2011) was perhaps the first dedicated and comprehensive statistical monograph on the topic. In the decade (almost) since the publication of that book, there has been an exponential increase in the number of papers dealing with spatio-temporal data analysis – not only in statistics, but also in many other branches of science. Although Cressie and Wikle (2011) is still extremely relevant, it was intended for a fairly advanced, technically trained audience, and it did not include software or coding examples. In contrast, the present book provides a more accessible introduction, with hands-on applications of the methods through the use of `R` Labs at the end of each chapter. At the time of writing, this unique aspect of the book fills a void in the literature that can provide a bridge for students and researchers alike who wish to learn the basics of spatio-temporal statistics.

What level is expected of readers of this book? First, although each chapter is fairly self-contained and they can be read in any order, we ordered the book deliberately to "ease" the reader into more technical material in later chapters. Spatio-temporal data can be complex, and their representations in terms of mathematical and statistical models can be complex as well. They require a number of indices (e.g., for space, for time, for multiple variables). In addition, being able to account for dependent random processes requires a bit of statistical sophistication that cannot be completely avoided, even in an applications-based introductory book. We believe that a reader who has taken a class or two in calculus-based probability and inference, and who is comfortable with basic matrix-algebra representations of statistical models (e.g., a multiple regression or a multivariate time-series representation), could comfortably get through this book. For those who would like a brief refresher on matrix algebra, we provide an overview of the components that we use in an appendix. To make this a bit easier on readers with just a few statistics courses on their transcript, we have interspersed "technical notes" throughout the book that provide short, gentle reviews of methods and ideas from the broader statistical literature.

Chapter 1 is the place to start, to get you intrigued and perhaps even excited about what is to come. We organized the rest of the book to follow what we believe to be good statistical practice. First, look at your data and do exploratory analyses (Chapter 2), then fit simple statistical models to the data to indicate possible patterns and see if assumptions are violated (Chapter 3), and then use what you learned in these analyses to build a spatio-temporal model that allows valid inferences (Chapters 4 and 5). The end of the cycle is to evaluate your model formally to find areas of improvement and to help choose the best model possible (Chapter 6). Then, if needed, repeat with a better-informed spatio-temporal model.

The bulk of the material on spatio-temporal modeling appears in Chapters 4 and 5. Chapter 4 covers descriptive (*marginal*) models formed by characterizing the spatio-temporal dependence structure (mainly through spatio-temporal covariances), which in turn leads to models that are analogous to the ubiquitous geostatistical models used in kriging. Chapter 5 focuses on dynamic (*conditional*) models that characterize the dynamic evolution of spatial processes through time, analogous to multivariate time-series models. Like Cressie and Wikle (2011), both Chapters 4 and 5 are firmly rooted in the notion of *hierarchical thinking* (i.e., hierarchical statistical modeling), which makes a clear distinction between the data and the underlying latent process of interest. This is based on the very practical notion that "[w]hat you see (data) is not always what you want to get (process)" (Cressie and Wikle, 2011, p. xvi).

Spatio-temporal statistics is such a vast field and this modestly sized book is necessarily not comprehensive. For example, we focus primarily on data whose spatial reference is a point, and we do not explore issues related to the "change-of-support" problem, nor do we deal with spatio-temporal point processes. Further, we mostly limit our discussion to models and methodologies that are relatively mature, understood, and widely used. Some of the applications our readers are confronted with will undoubtedly require cutting-edge methods beyond the scope of this book. In that regard, the book provides a down-to-earth introduction. We hope you find that the path is wide and the slope is gentle, ultimately giving you the confidence to explore the literature for new developments. For this reason, we have named our epilogical chapter *Pergimus*, Latin for "let us continue to progress."

A substantial portion of this book is devoted to "Labs," which enable the reader to put his or her understanding into practice using the programming language `R`. There are several reasons why we chose `R`: it is one of the most versatile languages designed for statistics; it is open source; it enjoys a vibrant online community whose members post solutions to virtually any problem you will encounter when coding; and, most importantly, a large number of packages that can be used for spatio-temporal modeling, exploratory data analysis, and statistical inference (estimation, prediction, uncertainty quantification, and so forth) are written in `R`. The last point is crucial, as it was our aim right from the beginning to make use of as much tried-and-tested code as possible to reduce the analyst's barrier to entry. Indeed, it is fair to say that this book would not have been possible without the excellent work, openness, and generosity of the `R` community as a whole.

In presenting the Labs, we intentionally use a "code-after-methodology" approach, since we firmly believe that the reader should have an understanding of the statistical methods being used before delving into the computational details. To facilitate the connections between methodology and computation, we have added "`R` Tips" where needed. The Labs themselves assume some prior knowledge of `R` and, in particular, of the *tidyverse*, which is built on an underlying philosophy of how to deal with data and graphics. Readers who would like to know more can consult the excellent book by Wickham and Grolemund (2016) for background reading (freely available online).

Finally, our goal when we started this project was to help as many people as we could to start analyzing spatio-temporal data. Consequently, with the generous support of our editors at Chapman & Hall/CRC, we have made the `.pdf` file of this book and the accompanying `R` package, **STRbook**, freely available for download from the website listed below. In addition, this website is a place where users can post *errata*, comment on the code examples, post their own code for different problems, their own spatio-temporal data sets, and articles on spatio-temporal statistics. You are invited to go to:

`https://spacetimewithr.org`

We hope you find this book useful for your endeavors as you begin to explore the complexities of the spatio-temporal world around us – and within us! Let's get started . . .

Christopher K. Wikle
Columbia, Missouri, USA

Andrew Zammit-Mangion
Wollongong, NSW, Australia

Noel Cressie
Wollongong, NSW, Australia

Chapter 1

Introduction to Spatio-Temporal Statistics

"I feel all things as dynamic events, being, changing, and interacting with each other in space and time even as I photograph them." (Wynn Bullock, 1902–1975, American photographer)

Wynn Bullock was an early pioneer of modern photography, and this quote captures the essence of what we are trying to get across in our book – except in our case the "photographs" are fuzzy and the pictures are incomplete! The top panel of Figure 1.1 shows the July 2014 launch of the US National Aeronautics and Space Administration (NASA) *Orbiting Carbon Observatory-2* (OCO-2) satellite, and the bottom panel shows the "photographer" in action. OCO-2 reached orbit successfully and, at the time of writing, is taking pictures of the dynamic world below. They are taken every fraction of a second, and each "photograph" is made up of measurements of the sun's energy in selected spectral bands, reflected from Earth's surface.

After NASA processes these measurements, an estimate is obtained of the fraction of carbon dioxide (CO_2) molecules in an atmospheric column between Earth's surface and the OCO-2 satellite. The top panel of Figure 1.2 shows these estimates in the boreal winter at locations determined by the geometry of the satellite's 16-day repeat cycle (the time interval after which the satellite retraces its orbital path). (They are color-coded according to their value in units of parts per million, or ppm.) Plainly, there are gaps caused by OCO-2's orbit geometry, and notice that the higher northern latitudes have very few data (caused by the sun's low angle at that time of the year). The bottom panel of Figure 1.2 shows 16 days of OCO-2 data obtained six months later, in the boreal summer, where the same comments about coverage apply, except that now the higher southern latitudes have very few data. Data incompleteness here is a moving target in both space and time. Furthermore, any color-coded "dot" on the map represents a datum that should not be totally believed, since

Figure 1.1: Top: Launch of NASA's OCO-2 satellite, on 02 July 2014 (credit: NASA/JPL). Bottom: An artist's impression of the OCO-2 satellite in orbit (credit: NASA/JPL).

it is an estimate obtained from measurements made through 700 km of atmosphere with clouds, water vapor, and dust getting in the way. That is, there is "noise" in the data.

There is a "+" on the global maps shown in Figure 1.2, which is at the location of the Mauna Loa volcano, Hawaii. Near the top of this volcano, at an altitude of 4.17 km, is the US National Oceanic and Atmospheric Administration (NOAA) Mauna Loa Observatory that has been taking monthly measurements of CO_2 since the late 1950s. The data are shown as a time series in Figure 1.3. Now, for the moment, put aside issues associated with measurements being taken with different instruments, on different parcels of air, at different locations, and for different blocks of time; these can be dealt with using quite

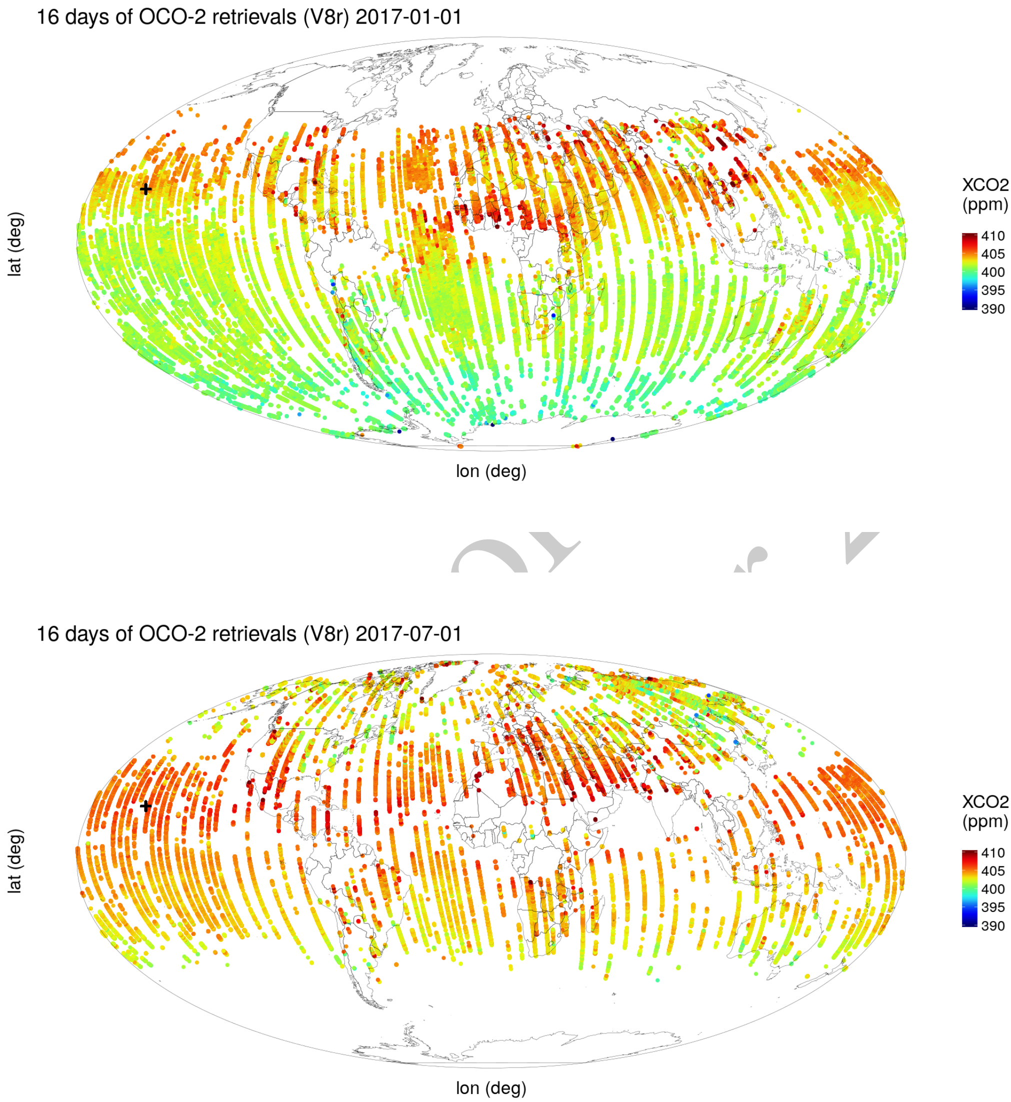

Figure 1.2: Sixteen days of CO_2 data from the OCO-2 satellite. Top: Data from 25 December 2016 to 09 January 2017 (boreal winter). Bottom: Data from 24 June 2017 to 09 July 2017 (boreal summer). The panel titles identify the eighth day of the 16-day window.

advanced spatio-temporal statistical methodology found in, for example, Cressie and Wikle (2011). What is fundamental here is that underlying these imperfect observations is a spatio-temporal process that itself is not perfectly understood, and we propose to capture this uncertainty in the process with a spatio-temporal statistical model.

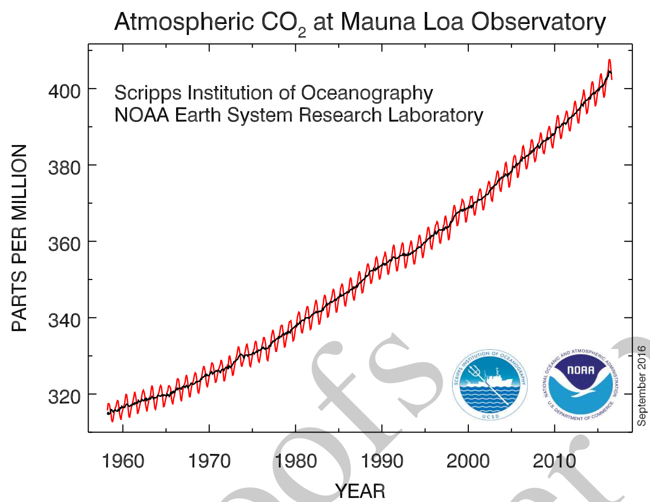

Figure 1.3: Monthly mean atmospheric CO_2 (ppm) at the NOAA Mauna Loa Observatory, Hawaii. The smooth line represents seasonally corrected data (Credit: Scripps Institution of Oceanography and NOAA Earth System Research Laboratory).

The atmospheric CO_2 process varies in space and in time, but the extent of its spatio-temporal domain means that exhaustive measurement of it is not possible; and even if it were possible, it would not be a good use of resources (a conclusion you should find evident after reading our book). Figure 1.2 shows two spatial views during short time periods that are six months apart; that is, it gives two spatial "snapshots." Figure 1.3 shows a temporal view at one particular location as it varies monthly over a 50-year time period; that is, it gives a temporal "profile." This is a generic problem in spatio-temporal statistics, namely our noisy data traverse different paths through the "space-time cube," but we want to gain knowledge about unobserved (and even observed) parts of it. We shall address this problem in the chapters, the Labs, and the technical notes that follow, drawing on a number of data sets introduced in Chapter 2.

Humans have a longing to understand their place (temporally and spatially) in the universe. In an Einsteinian universe, space and time interact in a special, "curved" way; however, in this book our methodology and applications are for a Newtonian world. Rick Delmonico, author of the book, *The Philosophy of Fractals* (Delmonico, 2017), has been quoted elsewhere as saying that "light is time at maximum compression and matter is space at maximum compression." Our Newtonian world is definitely more relaxed than this! Nevertheless, it is fascinating that images of electron motion at a scale of 10^{-11} meters look very much like images of the cosmos at a scale of 10^{17} meters (Morrison and Morrison, 1982).

Trying to understand spatio-temporal data and how (and ultimately why) they vary in space and time is not new – just consider trying to describe the growth and decline of populations, the territorial expansion and contraction of empires, the spread of world religions, species (including human) migrations, the dynamics of epidemics, and so on. Indeed, history and geography are inseparable. From this "big picture" point of view, there is a complex system of interacting physical, biological, and social processes across a range of spatial/temporal scales.

How does one do spatio-temporal statistics? Well, it is not enough to consider just spatial snapshots of a process at a given time, nor just time-series profiles at a given spatial location – the behavior at spatial locations at one time point will almost certainly affect the behavior at nearby spatial locations at the next time point. Only by considering time and space together can we address how spatially coherent entities change over time or, in some cases, why they change. It turns out that a big part of the *how* and *why* of such change is due to *interactions* across space and time, and across multiple processes.

For example, consider an influenza epidemic, which is generally in the winter season. Individuals in the population at risk can be classified as susceptible (S), infected (I), or recovered (R), and a well-known class of multivariate temporal models, called SIR models, capture the transition of susceptibles to infecteds to recovereds and then possibly back to susceptibles. At a micro level, infection occurs in the household, in the workplace, and in public places due to the interaction (contact) between infected and susceptible individuals. At a macro level, infection and recovery rates can be tracked and fitted to an SIR model that might also account for the weather, demographics, and vaccination rates. Now suppose we can disaggregate the total-population SIR rates into health-district SIR rates. This creates a spatio-temporal data set, albeit at a coarse spatial scale, and the SIR rates can be visualized dynamically on a map of the health districts. Spatio-temporal interactions may then become apparent, and the first steps of spatio-temporal modeling can be taken.

Spatio-temporal interactions are not limited to similar types of processes nor to spatial and temporal scales of variability that seem obvious. For example, El Niño and La Niña phenomena in the tropical Pacific Ocean correspond to periods of warmer-than-normal and colder-than-normal sea surface temperatures (SST), respectively. These SST "events" occur every two to seven years, although the exact timing of their appearance and their end is not regular. But it is well known that they have a tremendous impact on the weather across the globe, and weather affects a great number of things! For example, the El Niño and La Niña events can affect the temperature and rainfall over the midwest USA, which can affect, say, the soil moisture in the state of Iowa, which would likely affect corn production and could lead to a stressed US agro-economy during that period. Simultaneously, these El Niño and La Niña events can also affect the probability of tornado outbreaks in the famed "tornado alley" region of the central USA, and they can even affect the breeding populations of waterfowl in the USA.

Doing some clever smoothing and sharp visualizations of the spatial, temporal, and spatio-temporal variability in the data is a great start. But the information we glean from these data analyses needs to be organized, and this is done through models. In the next section, we make the case for spatio-temporal models that are *statistical*.

1.1 Why Should Spatio-Temporal Models Be *Statistical?*

In the physical world, phenomena evolve in space and time following deterministic, perhaps "chaotic," physical rules (except at the quantum level), so why do we need to consider randomness and uncertainty? The primary reason comes from the uncertainty resulting from incomplete knowledge of the science and of the mechanisms driving a spatio-temporal phenomenon. In particular, *statistical* spatio-temporal models give us the ability to model components in a physical system that appear to be random and, even if they are not, the models are useful if they result in accurate and precise predictions. Such models introduce the notion of uncertainty, but they are able to do so without obscuring the salient trends or regularities of the underlying process (that are typically of primary interest).

Take, for instance, the raindrops falling on a surface; to predict exactly where and when each drop will fall would require an inconceivably complex, deterministic, meteorological model, incorporating air pressure, wind speed, water-droplet formation, and so on. A model of this sort at a large spatial scale is not only infeasible but also unnecessary for many purposes. By studying the temporal intensity of drops on a regular spatial grid, one can test for spatio-temporal interaction or look for dynamic changes in spatial intensity (given in units of "per area") for each cell of the grid. The way in which the intensity evolves over time may reveal something about the driving mechanisms (e.g., wind vectors) and be useful for prediction, even though the exact location and time of each incident raindrop is uncertain.

Spatio-temporal statistical models are *not* at odds with deterministic ones. Indeed, the most powerful (in terms of predictive performance) spatio-temporal statistical models are those that are constructed based on an understanding of the biological or physical mechanisms that give rise to spatio-temporal variability and interactions. Hence, we sometimes refer to them as *physical-statistical models* (see the editorial by Kuhnert, 2014), or generally as *mechanistically motivated statistical models*. To this understanding, we add the reality that observations may have large gaps between them (in space and in time), they are observed with error, our understanding of the physical mechanisms is incomplete, we have limited knowledge about model parameters, and so on. Then it becomes clear that incorporating statistical distributions into the model is a very natural way to solve complex problems. Answers to the problems come as estimates or predictions along with a quantification of their uncertainties. These physical-statistical models, in the temporal domain, the spatial domain, and the spatio-temporal domain, have immense use in everything from anthropology to zoology and all the "ologies" in-between.

1.2 Goals of Spatio-Temporal Statistics

What are we trying to accomplish with spatio-temporal data analysis and statistical modeling? Sometimes we are just trying to gain more understanding of our data. We might be interested in looking for relationships between two spatio-temporally varying processes, such as temperature and rainfall. This can be as simple as visualizing the data or exploring them through various summaries (Chapter 2). Augmenting these data with scientific theories and statistical methodologies allows valid inferences to be made (Chapter 3). For example, successive reports from the United Nations Intergovernmental Panel on Climate Change have concluded from theory and data that a build-up of atmospheric CO_2 leads to a greenhouse effect that results in global warming. Models can then be built to answer more focused questions. For example, the CO_2 data shown in Figure 1.2 are a manifestation of Earth's carbon cycle: can we find precisely the spatio-temporal "places" on Earth's surface where carbon moves in and out of the atmosphere? Or, how might this warming affect our ability to predict whether an El Niño event will occur within 6 months?

Broadly speaking, there are three main goals that one might pursue with a spatio-temporal statistical model: (1) prediction in space and time (filtering and smoothing); (2) inference on parameters; and (3) forecasting in time. More specific goals might include data assimilation, computer-model emulation, and design of spatio-temporal monitoring networks. These are all related through the presence of a spatio-temporal statistical model, but they have their own nuances and may require different methodologies (Chapters 4 and 5).

1.2.1 The Two Ds of Spatio-Temporal Statistical Modeling

There have been two approaches to spatio-temporal statistical modeling that address the goals listed above. These are the "two Ds" referred to in the title of this subsection, namely the *descriptive* approach and the *dynamic* approach. Both are trying to capture statistical dependencies in spatio-temporal phenomena, but they go about it in quite different ways.

Probably the simplest example of this is in time-series modeling. Suppose that the dependence between any two data at different time points is modeled with a stationary first-order autoregressive process (AR(1)). *Dynamically*, the model says that the value at the current time is equal to a "propagation factor" (or "transition factor") times the value at the previous time, plus an independent "innovation error." This is a mechanistic way of presenting the model that is easy to simulate and easy to interpret.

Descriptively, the same probability structure can be obtained by defining the correlation between two values at any two given time points to be an exponentially decreasing function of the lag between the two time points. (The rate of decrease depends on the AR(1) propagation factor.) Viewing the model this way, it is not immediately obvious how to simulate from it nor what the behavior of the correlation function means physically.

The "take-home" here is that, while there is a single underlying probability model common to the two specifications, the dynamic approach has some attractive interpretable features that the descriptive approach does not have. Nevertheless, in the absence of knowledge of the dynamics, it can be the descriptive approach that is more "fit for purpose." With mean and covariance functions that are sufficiently flexible, a good fit to the data can be obtained and, consequently, the spatio-temporal variability can be well described.

1.2.2 Descriptive Modeling

The descriptive approach typically seeks to characterize the spatio-temporal process in terms of its mean function and its covariance function. When these are sufficient to describe the process, we can use "optimal prediction" theory to obtain predictions and, crucially, their associated prediction uncertainties. This approach has a distinguished history in spatial statistics and is the foundation of the famed *kriging* methodology. (Cressie, 1990, presents the early history of kriging.) In a spatio-temporal setting, the descriptive approach is most useful when we do not have a strong understanding of the mechanisms that drive the spatio-temporal phenomenon being modeled. Or perhaps we are more interested in studying how covariates in a regression are influencing the phenomenon, but we also recognize that the errors that occur when fitting that relationship are statistically dependent in space and time. That is, the standard assumption given in Chapter 3, that errors are independent and identically distributed (iid), is *not* tenable. In this case, knowing spatio-temporal covariances between the data is enough for statistically efficient inferences (via generalized least squares) on regression coefficients (see Chapter 4). But, as you might suspect, it can be quite difficult to specify all possible covariances for complex spatio-temporal phenomena (and, for nonlinear processes, covariances are not sufficient to describe the spatio-temporal statistical dependence within the process).

Sometimes we can describe spatio-temporal dependence in a phenomenon by including in our model covariates that capture spatio-temporal "trends." This large-scale spatio-temporal variability leaves behind smaller-scale variability that can be modeled statistically with spatio-temporal covariances. The descriptive approach often relies on an important statistical characteristic of dependent data, namely that nearby (in space and time) observations tend to be more alike than those far apart. In spatial modeling, this is often referred to as "Tobler's first law of geography" (Tobler, 1970), and it is often a good guiding principle. It is fair to point out, though, that there are exceptions: there might be "competition" (e.g., only smaller trees are likely to grow close to or under bigger trees as they compete over time for light and nutrients), or things may be more alike on two distant mountain peaks at the same elevation than they are on the same mountain peak at different elevations.

It is important to take a look back at the writings of the pioneers in statistics and ask why spatio-temporal statistical dependencies were not present in early statistical models if they are so ubiquitous in real-world data. Well, we know that some people definitely were aware of these issues. For example, in his ground-breaking treatise on the design of experiments in agriculture, R. A. Fisher (1935, p. 66) wrote: "After choosing the area we usually have no guidance beyond the widely verified fact that patches in close proximity are commonly more alike, as judged by the yield of crops, than those which are further apart." In this case, the spatial variability between plots is primarily due to the fact that the soil properties vary relatively smoothly across space at the field level. Unfortunately, Fisher could not implement complex error models that included spatial statistical dependence due to modeling and computational limitations at that time. So he came up with the brilliant solution of introducing randomization into the experimental design in order to avoid confounding plot effects and treatment effects (but note, only at the plot scale). This was one of the most important innovations in twentieth-century science, and it revolutionized experimentation, not only in agriculture but also in industrial and medical applications. Readers interested in more details behind the development of spatial and spatio-temporal statistics could consult Chapter 1 of Cressie (1993) and Chapter 1 of Cressie and Wikle (2011), respectively.

1.2.3 Dynamic Modeling

Dynamic modeling in the context of spatio-temporal data is simply the notion that we build statistical models that posit (either probabilistically or mechanistically) how a spatial process changes through time. It is inherently a conditional approach, in that we condition on knowing the past, and then we model how the past statistically evolves into the present. If the spatio-temporal phenomenon is what we call "stationary," we could take what we know about it in the present (and the past) and forecast what it will look like in the future.

Building spatio-temporal models using the dynamic approach is closer to how scientists think about the etiology of processes they study – that is, most spatio-temporal data *really do* correspond to a mechanistic real-world process that can be thought of as a spatial process evolving through time. This connection to the mechanism of the process allows spatio-temporal dynamic models a better chance to establish answers to the "why" questions (causality) – is this not the ultimate goal of science? Yet, there is no free lunch – the power of these models comes from established knowledge about the process's behavior, which may not be available for the problem at hand. In that case, one might specify more flexible classes of dynamic models that can adapt to various types of evolution, or turn to the descriptive approach and fit flexible mean and covariance functions to the data.

From a statistical perspective, dynamic models are closer to the kinds of statistical models studied in time series than to those studied in spatial statistics. Yet, there are two fundamental differences between spatio-temporal statistical models that are dynamic, and the usual multivariate time-series models. The first is that dynamic spatio-temporal models have to represent realistically the kinds of spatio-temporal interactions that take place in the phenomenon being studied – not all relationships that one might put into a multivariate time-series model make physical (or biological or economic or ...) sense. The second reason has to do with dimensionality. It is very often the case in spatio-temporal applications that the dimensionality of the spatial component of the model prohibits standard inferential methods. That is, there would be too much "multi" if one chose a multivariate time-series representation of the phenomenon. Special care has to be taken as to how the model is parameterized in order to obtain realistic yet parsimonious dynamics. As discussed in Chapter 5, this has been facilitated to a large extent by the development of basis function expansions within hierarchical statistical models.

Irrespective of which "D" is used to model a spatio-temporal data set, its sheer size can overwhelm computations. Model formulations that use basis functions are a powerful way to leap-frog the computational bottleneck caused by inverting a very large covariance matrix of the data. The general idea is to represent a spatio-temporal process as a mixed linear model with known covariates whose coefficients are unknown and non-random, together with known basis functions whose coefficients are unknown and *random* (Chapters 4 and 5). Usually the basis functions are functions of space and their coefficients define a multivariate time series of dependent random vectors. Depending on the type of basis functions considered, this formulation gives computational advantages due to reduced dimensions and/or sparse covariance/precision matrices that facilitate or eliminate the need for matrix inversions.

There are many classes of basis functions to choose from (e.g., Fourier, wavelets, bisquares) and many are multi-resolutional, although physically based functions (e.g., elevation) can easily be added to the class. If the basis functions are spatial and their random coefficients depend only on time, then the temporal dependence of the coefficients can capture complex spatio-temporal interactions. These include phenomena for which fine spatial scales affect coarse spatial scales and, importantly, vice versa.

1.3 Hierarchical Statistical Models

We believe that we are seeing the end of the era of constructing marginal-probability-based models for complex data. Such models are typically based on the specification of likelihoods from which unknown parameters are estimated. However, these likelihoods can be extremely difficult (or impossible) to compute when there are complex dependencies, and they cannot easily deal with the reality that the data are noisy versions of an underlying real-world process that we care about.

An alternative way to introduce statistical uncertainty into a model is to think conditionally and build complexity through a series of conditional-probability models. For example, if most of the complex dependencies in the data are due to the underlying process of interest, then one should model the distribution of the data *conditioned* on that process (data model), followed by a model of the process' behavior and its uncertainties (process model). There will typically be unknown parameters present, in both the statistical model for the data (conditioned on the process) and the statistical model for the process.

When a dynamic model of one or several variables is placed within a hierarchical model formulation (see below), one obtains what has been historically called a *state-space model* in the time-series literature. That is, one has data that are collected sequentially in time (i.e., a time series), and they are modeled as "noisy" observations of an underlying *state process* evolving (statistically) through time. These models are at the core of a number of engineering applications (e.g., space missions), and the challenge is to find efficient approaches to perform inference on the underlying state process of interest while accounting for the noise.

In general, there are three such situations of interest when considering state-space models: *smoothing, filtering*, and *forecasting*. *Smoothing* refers to inference on the hidden state process during a fixed time period in which we have observations throughout the time period. (The reader might note that this is the temporal analog of spatial prediction on a bounded spatial domain.) Now consider a time period that always includes the most current time, at which the latest observation is available. *Filtering* refers to inference on the hidden state value at the most current time based on the current and all past data. The most famous example of filtering in this setting is a methodology known widely as the Kalman filter (Kalman, 1960). Finally, *forecasting* refers to inference on the hidden state value at any time point beyond the current time, where data are either not available or not considered in the forecast. In this book, instead of modeling the evolution of a single variable or several variables, we model entire spatial processes evolving through time, which often adds an extra layer of modeling complexity and computational difficulty. Chapter 5 discusses how basis-function representations can deal with these difficulties.

In addition to uncertainty associated with the data and the underlying spatio-temporal process, there might be uncertainties in the parameters. These uncertainties could be accounted for statistically by putting a prior distribution on the parameters. To make sense of all this, we use *hierarchical (statistical) models* (HMs), and follow the terminology of Berliner (1996), who defined an HM to include a *data model*, a *process model*, and a *parameter model*. Technical Note 1.1 gives the conditional-probability structure that ties these models together into a coherent joint probability of all the uncertainties. The key to the Berliner HM framework is that, at any level of a spatio-temporal HM, it is a good strategy to put as much of the dependence structure as possible in the conditional-mean specification in order to simplify the conditional-covariance specification.

When the parameters are given prior distributions (i.e., a parameter model is posited) at the bottom level of the hierarchy, then we say that the model is a *Bayesian hierarchical model* (BHM). A BHM is often necessary for complex-modeling situations, because the parameters themselves may exhibit quite complex (e.g., spatial or temporal) structure. Or they may depend on other covariates and hence could be considered as processes in their own right. In simpler models, an alternative approach is to estimate the parameters present in the top two levels in some way using the data or other sources of data; then we like to say that the hierarchical model is an *empirical hierarchical model* (EHM). When applicable, an EHM may be preferred if the modeler is reluctant to put prior distributions on parameters about which little is known, or if computational efficiencies can be gained.

It is clear that the BHM approach allows very complex processes to be modeled by going deeper and deeper in the hierarchy, but at each level the conditional-probability model can be quite simple. Machine learning uses a similar approach with its *deep models*. A cascade of levels, where the processing of output from the previous level is relatively simple, results in a class of machine-learning algorithms known as *deep learning*. A potential advantage of the BHM approach over deep learning is that it provides a unified probabilistic framework that allows one to account for uncertainty in data, model, and parameters.

A very important advantage of the data–process–parameter modeling paradigm in an HM is that, while marginal-dependence structures are difficult to model directly, conditional-dependence structures usually come naturally. For example, it is often reasonable to assume that the *data covariance matrix* (given the corresponding values of the hidden process) is simply a diagonal matrix of measurement-error variances. This frees up the *process covariance matrix* to capture the "pure" spatio-temporal dependence, ideally (but, not necessarily) from physical or mechanistic knowledge. Armed with these two covariance matrices, the seemingly complex *marginal covariance matrix* of the data can be simply obtained. This same idea is used in mixed-effects modeling (e.g., in longitudinal data analysis), and it is apparent in the spatio-temporal statistical models described in Chapters 4 and 5.

The product of the conditional-probability components of the HM gives the joint probability model for all random quantities (i.e., all "unknowns"). The HM could be either a BHM or an EHM, depending on whether, respectively, a prior distribution is put on the parameters (i.e., a parameter model is posited) or the parameters are estimated. (A hybrid situation arises when some but not all parameters are estimated and the remaining have a prior distribution put on them.) In this book, we are primarily interested in obtaining the (finite-dimensional) distribution of the hidden (discretized) spatio-temporal process given the data, which we call the *predictive distribution*. The BHM also allows one to obtain the posterior distribution of the parameters given the data, whereas the EHM requires an estimate of the parameters. Predictive and posterior distributions are obtained using *Bayes' Rule* (Technical Note 1.1).

Since predictive and posterior distributions must have total probability mass equal to 1, there is a critical normalizing constant to worry about. Generally, it cannot be calculated in closed form, in which case we rely on computational methods to deal with it. Important advances in the last 30 years have alleviated this problem by making use of Monte Carlo samplers from a Markov chain whose stationary distribution is the predictive (or the posterior) distribution of interest. These *Markov chain Monte Carlo* (MCMC) methods have revolutionized the use of HMs for complex modeling applications, such as those found in spatio-temporal statistics.

Technical Note 1.1: Berliner's Bayesian Hierarchical Model (BHM) paradigm

First, the fundamental notion of the *law of total probability* allows one to decompose a joint distribution into a series of conditional distributions: $[A, B, C] = [A \mid B, C][B \mid C][C]$, where the "bracket notation" is used to denote probability distributions; for example, $[A, B, C]$ is the *joint distribution* of random variables A, B, and C, and $[A \mid B, C]$ is the *conditional distribution* of A given B and C.

Mark Berliner's insight (Berliner, 1996) was that one should use this simple decomposition as a way to formulate models for complex dependent processes. That is, the joint distribution, [data, process, parameters], can be factored into three levels.

At the top level is the *data model*, which is a probability model that specifies the distribution of the data given an underlying "true" process (sometimes called the hidden or latent process) and given some parameters that are needed to specify this distribution. At the next level is the *process model*, which is a probability model that describes the hidden process (and, thus, its uncertainty) given some parameters. Note that at this level the model does not need to account for measurement uncertainty. The process model can then use science-based theoretical or empirical knowledge, which is often physical or mechanistic. At the bottom level is the parameter model, where uncertainty about the parameters is modeled. From top to bottom, the levels of a BHM are:

1. Data model: [data | process, parameters]
2. Process model: [process | parameters]
3. Parameter model: [parameters]

Importantly, each of these levels could have sub-levels, for which conditional-probability models could be given.

Ultimately, we are interested in the posterior distribution, [process, parameters | data] which, conveniently, is proportional to the product of the levels of the BHM given above:

$$
\begin{aligned}
[\text{process, parameters} \mid \text{data}] \;\propto\;& [\text{data} \mid \text{process, parameters}] \\
&\times [\text{process} \mid \text{parameters}] \\
&\times [\text{parameters}],
\end{aligned}
$$

where "$\propto$" means "is proportional to." (Dividing the right-hand side by the normalizing constant, [data], makes it equal to the left-hand side.) Note that this result comes from application of Bayes' Rule, applied to the hierarchical model. Inference based on complex models typically requires numerical evaluation of the posterior (e.g., MCMC methods), because the normalizing constant cannot generally be calculated in closed form.

An empirical hierarchical model (EHM) uses just the first two levels, from which the predictive distribution is

$$\begin{aligned}[\text{process} \mid \text{data, parameters}] \propto \; & [\text{data} \mid \text{process, parameters}] \\ & \times [\text{process} \mid \text{parameters}],\end{aligned}$$

where *parameter estimates* are substituted in for "parameters." Numerical evaluation of this (empirical) predictive distribution is also typically needed, since the EHM's normalizing constant cannot generally be calculated in closed form.

1.4 Structure of the Book

The remaining chapters in this book are arranged in the way that we often approach statistical modeling in general and spatio-temporal modeling in particular. That is, we begin by exploring our data. So, Chapter 2 gives ways to do this through visualization and through various summaries of the data. We note that both of these types of exploration can be tricky with spatio-temporal data, because we have one or more dimensions in space and one in time. It can be difficult to visualize information in more than two dimensions, so it often helps to slice through or aggregate over a dimension, or use color, or build animations through time. Similarly, when looking at numerical summaries of the data, we have to come up with innovative ways to help reduce the inherent dimensionality and to examine dependence structures and potential relationships in time and space.

After having explored our data, it is often the case that we would like to fit some fairly simple models – sometimes to help us do an initial filling-in of missing observations that will assist with further exploration, or sometimes just to see if we have enough covariates to adequately explain the important dependencies in the data. This is the spirit of Chapter 3, which presents some ways to do spatial prediction that are not based on a statistical model or are based on very basic statistical models that do not explicitly account for spatio-temporal structure (e.g., linear regression, generalized linear models, and generalized additive models).

If the standard models presented in Chapter 3 are not sufficient to accomplish the goals we gave in Section 1.2, what are we to do? This is when we start to consider the descriptive and dynamic approaches to spatio-temporal modeling discussed above. The descriptive approach has been the "workhorse" of spatio-temporal statistical modeling for most of the history of the discipline, and these methods (e.g., kriging) are described in Chapter 4. But, as mentioned above, when we have strong mechanistic knowledge about the underlying process and/or are interested in complex prediction or forecasting scenarios, we often benefit from the dynamic approach described in Chapter 5. Take note that Chapters 4 and 5 will require a bit more patience to go through, because process models that incorporate statistical dependence require more mathematical machinery. Hence, in these two chapters, the notation and motivation will be somewhat more technical than for the models presented in Chapter 3. It should be kept in mind, though, that the aim here is not to make you an expert, rather it is to introduce you (via the text, the Labs, and the technical notes) to the motivations, main concepts, and practicalities behind spatio-temporal statistical modeling.

After building a model, we would like to know how good it is. There are probably as many ways to evaluate models as there are models! So, it is safe to say that there is no standard way to evaluate a spatio-temporal statistical model. However, there are some common approaches that have been used in the past to carry out model evaluation and model comparison, some of which apply to spatio-temporal models (see Chapter 6). We note that the aim there is not to show you how to obtain the "best" model (as there isn't one!). Rather, it is to show you how a model or a set of models can be found that does a reasonable job with regard to the goals outlined in Section 1.2.

Last, but certainly not least, each of Chapters 2–6 contain Lab vignettes that go through the implementation of many of the important methods presented in each chapter using the `R` programming language. This book represents the first time such a comprehensive collection of `R` examples for spatio-temporal data have been collected in one place. We believe that it is essential to "get your hands dirty" with data, but we recognize that quite a few of the methods and approaches used in spatio-temporal statistics can be complicated and that it can be daunting to program them yourself from scratch. Therefore, we have tried to identify some useful (and stable) `R` functions from existing `R` packages (see the list following the appendices) that can be used to implement the methods discussed in Chapters 2–6. We have also put a few functions of our own, along with the data sets that we have used, in the `R` package, **STRbook**, associated with this book (instructions for obtaining this package are available at `https://spacetimewithr.org`). We note that there are many other `R` packages that implement various spatio-temporal methods, whose approaches could arrive at the same result with more or less effort, depending on familiarity. As is often the case with `R`, one gets used to doing things a certain way, and so most of our choices are representative of this.

Chapter 2

Exploring Spatio-Temporal Data

Exploration into territory unknown, or little known, requires both curiosity and survival skills. You need to know where you are, what you are looking at, and how it relates to what you have seen already. The aim of this chapter is to teach you those skills for exploring spatio-temporal data sets. The curiosity will come from you!

Spatio-temporal data are everywhere in science, engineering, business, and industry. This is driven to a large extent by various automated data acquisition instruments and software. In this chapter, after a brief introduction to the data sets considered in this book, we describe some basic components of spatio-temporal data structures in R, followed by spatio-temporal visualization and exploratory tools. The chapter concludes with fairly extensive Labs that provide examples of R commands for data wrangling, visualization, and exploratory data analysis.

When you discover the peaks and valleys, trends and seasonality, and changing landscapes in your data set, what then? Are they real or illusory? Are they important? Chapters 3–6 will give you the inferential and modeling skills required to answer these questions.

2.1 Spatio-Temporal Data

Time-series analysts consider univariate or multivariate sequential data as a random process observed at regular or irregular intervals, where the process can be defined in continuous time, discrete time, or where the temporal event is itself the random event (i.e., a *point process*). Spatial statisticians consider spatial data as either temporal aggregations or temporally frozen states ("snapshots") of a spatio-temporal process. Spatial data are traditionally thought of as random according to either *geostatistical*, *areal* or *lattice*, or *point process* (and sometimes *random set*) behavior. We think of geostatistical data as the kind where we could have observations of some variable or variables of interest (e.g., temperature and wind speed) at continuous locations over a given spatial domain, and where we seek to predict those variables at unknown locations in space (e.g., using interpolation methodology such as *kriging*). Lattice processes are defined on a finite or countable subset in space (e.g., grid nodes, pixels, polygons, small areas), such as the process defined by work-force indicators on a specific political geography (e.g., counties in the USA) over a specific period of time. A spatial point process is a stochastic process in which the locations of the points (sometimes called *events*) are random over the spatial domain, where these events can have attributes given in terms of *marks* (e.g., locations of trees in a forest are random events, with the diameter at breast height being the mark). Given the proliferation of various data sources and geographical information system (GIS) software, it is important to broaden the perspective of spatial data to include not only points and polygons, but also *lines*, *trajectories*, and *objects*. It is also important to note that there can be significant differences in the abundance of spatial information versus temporal information.

R tip: Space-time data are usually provided in comma-separated value (CSV) files, which can be read into `R` using **`read.csv`** or **`read.table`**; shapefiles, which can be read into `R` using functions from **rgdal** and **maptools**; NetCDF files, which can be read into `R` using a variety of packages, such as **ncdf4** and **RNetCDF**; and HDF5 files, which can be read into `R` using the package **h5**.

It should not be surprising that data from spatio-temporal processes can be considered from either a time-series perspective or a spatial-random-process perspective, as described in the previous paragraph. In this book, we shall primarily consider spatio-temporal data that can be described by processes that are discrete in time and either geostatistical or on a lattice in space. For a discussion of a broader collection of spatio-temporal processes, see Cressie and Wikle (2011), particularly Chapters 5–9.

Throughout this book, we consider the following data sets:

- *NOAA daily weather data.* These daily data originated from the US National Oceanic and Atmospheric Administration (NOAA) National Climatic Data Center and can be obtained from the IRI/LDEO Climate Data Library at Columbia University.[1] The data set we consider consists of four variables: daily maximum temperature (`Tmax`) in degrees Fahrenheit (°F), minimum temperature (`Tmin`) in °F, dew point temperature (`TDP`) in °F, and precipitation (`Precip`) in inches at 138 weather stations in the central USA (between 32°N–46°N and 80°W–100°W), recorded between the years 1990 and 1993 (inclusive). These data are considered to be discrete and regular in time (daily) and geostatistical and irregular in space. However, the data are not complete, in that there are missing measurements at various stations and at various time points, and the stations themselves are obviously not located everywhere in the central USA. We will refer to these data as the "NOAA data set." Three days of `Tmax` measurements from the NOAA data set are shown in Figure 2.1.

[1] `http://iridl.ldeo.columbia.edu/SOURCES/.NOAA/.NCDC/.DAILY/.FSOD/`

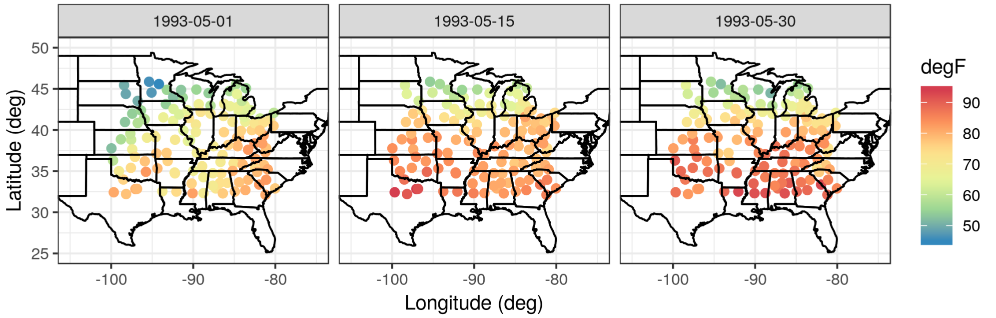

Figure 2.1: Maximum temperature (`Tmax`) in °F from the NOAA data set on 01, 15, and 30 May 1993.

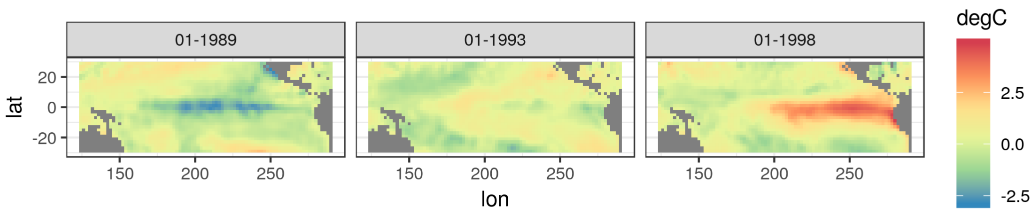

Figure 2.2: Sea-surface temperature anomalies in °C for the month of January in the years 1989, 1993, and 1998. The year 1989 experienced a La Niña event (colder than normal temperatures) while the year 1998 experienced an El Niño event (warmer than normal temperatures).

- *Sea-surface temperature anomalies*. These sea-surface temperature (SST) anomaly data are from the NOAA Climate Prediction Center as obtained from the IRI/LDEO Climate Data Library at Columbia University.[2] The data are gridded at a 2° by 2° resolution from 124°E–70°W and 30°S–30°N, and they represent monthly anomalies from a January 1970–December 2003 climatology (averaged over time). We refer to this data set as the "SST data set." Three individual months from the SST data set are shown in Figure 2.2.

- *Breeding Bird Survey (BBS) counts*. These data are from the North American Breeding Bird Survey.[3] In particular, we consider yearly counts of the house finch (*Carpodacus mexicanus*) at BBS routes for the period 1966–2000 and the Carolina wren

[2] `http://iridl.ldeo.columbia.edu/SOURCES/.CAC/`

[3] K. L. Pardieck, D. J. Ziolkowski Jr., M. Lutmerding, and M.-A. R. Hudson, US Geological Survey, Patux-

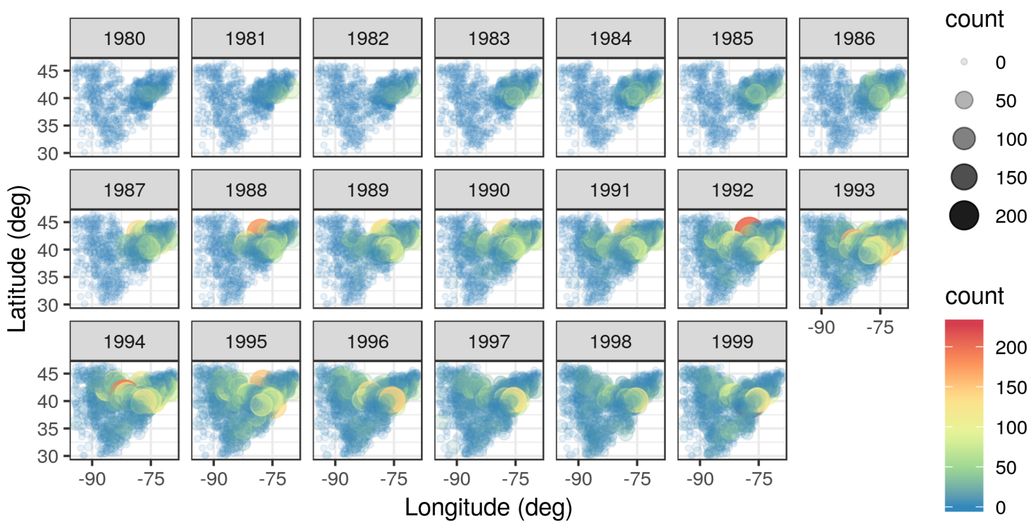

Figure 2.3: Counts of house finches between 1980 and 1999. The size of the points is proportional the number of observed birds, while transparency is used to draw attention to regions of high sampling density or high observed counts.

(*Thryothorus ludovicianus*) for the period 1967–2014. The BBS sampling unit is a roadside route of length approximately 39.2 km. In each sampling unit, volunteer observers make 50 stops and count birds for a period of 3 minutes when they run their routes (typically in June). There are over 4000 routes in the North American survey, but not all routes are available every year. For the purposes of the analyses in this book, we consider the total route counts to occur yearly (during the breeding season) and define the spatial location of each route to be the route's centroid. Thus, we consider the data to be discrete in time, geostatistical and irregular in space, and non-Gaussian in the sense that they are counts. We refer to this data set as the "BBS data set." Counts of house finches for the period 1980–1999 are shown in Figure 2.3.

- *Per capita personal income*. We consider yearly per capita personal income (in dollars) data from the US Bureau of Economic Analysis (BEA).[4] These data have areal spatial support corresponding to US counties in the state of Missouri, and they cover the period 1969–2014. We refer to this data set as the "BEA income data set." Figure 2.4 shows these data, on a log scale, for the individual years 1970, 1980, and

ent Wildlife Research Center (`https://www.pwrc.usgs.gov/bbs/RawData/`). Note that we used the archived 2016.0 version of the data set, doi: 10.5066/F7W0944J, which is accessible through the data archive link on the bbs website (`ftp://ftpext.usgs.gov/pub/er/md/laurel/BBS/Archivefiles/Version2016v0/`).

[4] `http://www.bea.gov/regional/downloadzip.cfm`

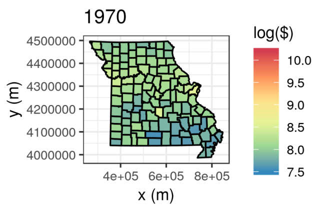

Figure 2.4: Per capita personal income (in dollars) by county for residents in Missouri in the years 1970, 1980, and 1990, plotted on a log scale. The data have been adjusted for inflation. Note how both the overall level of income as well as the spatial variation change with time.

1990; note that these data have been adjusted for inflation.

- *Sydney radar reflectivity*. These data are a subset of consecutive weather radar reflectivity images considered in the World Weather Research Programme (WWRP) Sydney 2000 Forecast Demonstration Project. There are 12 images at 10-minute intervals starting at 08:25 UTC on 03 November, 2000 (i.e., 08:25–10:15 UTC). The data were originally mapped to a 45×45 grid of 2.5 km pixels centered on the radar location. The data used in this book are for a region of dimension 28×40, corresponding to a 70 km by 100 km domain. All reflectivities are given in "decibels relative to Z" (dBZ, a dimensionless logarithmic unit used for weather radar reflectivities). We refer to this data set as the "Sydney radar data set." For more details on these data, shown in Figure 2.5, see Xu et al. (2005).

- *Mediterranean winds*. These data are east–west (u) and north–south (v) wind-component observations over the Mediterranean region (from -6.5°E–16.5°E and 33.5°N–45.5°N) for 28 time periods (every 6 hours) from 00:00 UTC on 29 January 2005 to 18:00 UTC on 04 February 2005. There are two data sources: satellite wind observations from the QuikSCAT scatterometer, and surface winds and pressures from an analysis by the European Center for Medium Range Weather Forecasting (ECMWF). The ECMWF-analysis winds and pressures are given on a $0.5° \times 0.5°$ spatial grid (corresponding to 47 longitude locations and 25 latitude locations), and they are available at each time period for all locations. The QuikSCAT observations are only available intermittently in space, due to the polar orbit of the satellite, but at much higher spatial resolution (25 km) than the ECMWF data when they are available. The QuikSCAT observations given for each time period correspond to all observations available in the spatial domain within 3 hours of time periods stated above. There are no QuikSCAT observations available at 00:00 UTC and 12:00 UTC in the spatial domain and time periods considered here. We refer to this data set as the "Mediterranean winds data set." Figure 2.6 shows the wind vectors ("quivers")

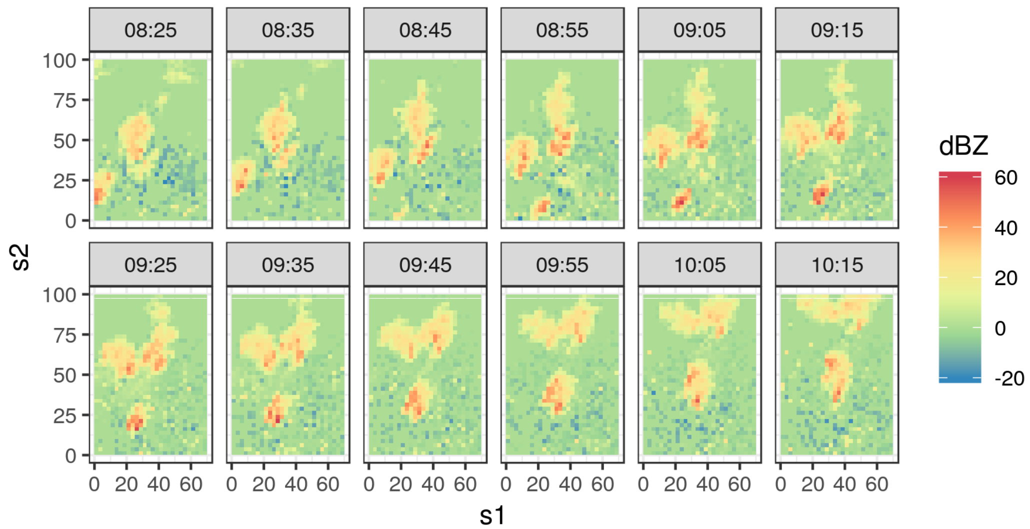

Figure 2.5: Weather radar reflectivities in dBZ for Sydney, Australia, on 03 November 2000. The images correspond to consecutive 10-minute time intervals from 08:25 UTC to 10:15 UTC.

for the ECMWF data at 06:00 UTC on 01 February 2005. These data are a subset of the data described in Cressie and Wikle (2011, Chapter 9) and Milliff et al. (2011).

2.2 Representation of Spatio-Temporal Data in R

Although there are many ways to represent spatial data and time-series data in R, there are relatively few ways to represent spatio-temporal data. In this book we use the class definitions defined in the R package **spacetime**. These classes extend those used for spatial data in **sp** and time-series data in **xts**. For details, we refer the interested reader to the package documentation and vignettes in Pebesma (2012). Here, we just provide a brief introduction to some of the concepts that facilitate thinking about spatio-temporal data structures.

Although spatio-temporal data can come in quite sophisticated relational forms, they most often come in the form of fairly simple "tables." Pebesma (2012) classifies these simple tables into three classes:

- *time-wide*, where columns correspond to different time points;

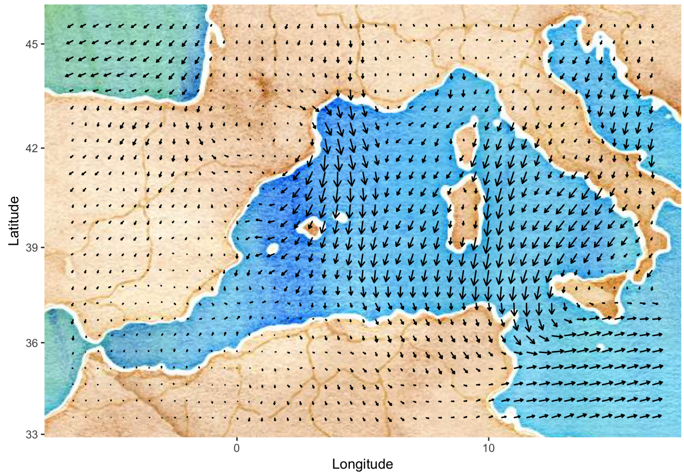

Figure 2.6: ECMWF wind vector observations over the Mediterranean region for 06:00 UTC on 01 February 2005.

- *space-wide*, where columns correspond to different spatial features (e.g., locations, regions, grid points, pixels);
- *long formats*, where each record corresponds to a specific time and space coordinate.

R tip: Data in long format are space inefficient, as spatial coordinates and time attributes are required for each data point, whether or not data are on a lattice. However, it is easy to subset and manipulate data in long format. Powerful "data wrangling" tools in packages such as **dplyr** and **tidyr**, and visualization tools in **ggplot2**, are designed for data in long format.

Tables are very useful elementary data objects. However, an object from the **spacetime** package contains additional information, such as the map projection and the time zone. Polygon objects may further contain the individual areas of the polygons as well as the individual bounding boxes. These objects have elaborate, but consistent, class definitions that greatly aid the geographical (e.g., spatial) component of the analysis.

Pebesma (2012) considers four classes of space-time data:

- *full grid* (`STF`), a combination of any **sp** object and any **xts** object to represent all possible locations on the implied space-time lattice;

- *sparse grid* (`STS`), as `STF`, but contains only the non-missing space-time combinations on a space-time lattice;
- *irregular* (`STI`), an irregular space-time data structure, where each point is allocated a spatial coordinate and a time stamp;
- *simple trajectories* (`STT`), a sequence of space-time points that form trajectories.

Note that the "grid" in the first two classes corresponds to a *space-time lattice* – but the spatial locations may or may not be on a lattice! The sparse grid is most effective when there are missing observations, or when there are a relatively few spatial locations that have different time stamps, or when there are a relatively small number of times that have differing spatial locations.

It is important to note that the class objects that make up the **spacetime** package are not used to store data; this is accomplished through the use of the `R` data frame. As illustrated in Lab 2.1 at the end of this chapter and in Pebesma (2012), there are several important methods in **sp** and **spacetime** that help with the construction and manipulation of these spatio-temporal data sets. In particular, there are methods to construct an object, replace/select data or various spatial or temporal subsets, coerce spatio-temporal objects to other classes, overlay spatio-temporal observations, and aggregate over space, time, or space-time.

> **`R` tip:** When spatio-temporal data have non-trivial support (i.e., a spatio-temporal region over which a datum is defined), and if the geometry allows it, use **SpatialPixels** and not **SpatialPolygons** as the underlying **sp** object. This results in faster geometric manipulations such as when finding the overlap between points and polygons using the function `over`.

2.3 Visualization of Spatio-Temporal Data

A picture – or a video – can be worth a thousand tables. Use of maps, color, and animation is a very powerful way to provide insight that suggests exploratory data analysis that then leads to spatio-temporal models (Chapters 3–5). Although there are distinct challenges in visualizing spatio-temporal data due to the fact that several dimensions often have to be considered simultaneously (e.g., two or three spatial dimensions and time), there are some fairly common tools that can help explore such data visually. For the most part, we are somewhat selective in what we present here as we want to convey fairly simple methods that have consistently proven useful in our own work and in the broader literature. These can be as simple as static spatial maps and time-series plots, or they can be interactive explorations of the data. In addition, because of the special dynamic component of many spatio-temporal processes, where spatial processes evolve through time, it is often quite useful to try to visualize this evolution. This can be done in the context of one-dimensional space through a space-time (*Hovmöller*) plot, or more generally through *animations*. We conclude by discussing an increasingly popular approach to help with visualization of very high-dimensional data.

R tip: Spatio-temporal visualization in `R` generally proceeds using one of two methods: the trellis graph or the grammar of graphics. The command `plot` invokes the trellis graph when **sp** or **spacetime** objects are supplied as arguments. The commands associated with the package **ggplot2** invoke the grammar of graphics. The data objects frequently need to be converted into a data frame in long format for use with **ggplot2**, which we often use throughout this book.

2.3.1 Spatial Plots

Snapshots of spatial processes for a given time period can be plotted in numerous ways. If the observations are irregular in space, then it is often useful to plot a symbol at the data location and give it a different color and/or size to reflect the value of the observation. For example, consider `Tmax` for 01 May 1993 from the NOAA data set plotted in the left panel of Figure 2.1. In this case, the circle center corresponds to the measurement location and the color of the filled-in circle corresponds to the value of the maximum temperature. Notice the clear visual trend of decreasing temperatures from the southeast to the northwest over this region of the USA.

Spatial plots of gridded data are often presented as contour plots, so-called "image" plots, or surface plots. For example, Figure 2.2 shows image representations for three individual months of the Pacific SST data set. Note the La Niña signal (cooler than normal SSTs) in 1989 and the El Niño signal (warmer than normal SSTs) in 1998 in the tropical Pacific Ocean. Figure 2.7 shows contour and surface representations of the SST anomalies in January 1998, corresponding to the right panel (i.e., the El Niño event) in Figure 2.2.

It is often useful to plot a sequence of spatial maps for consecutive times to gain greater insight into the *changes in* spatial patterns through time. Figure 2.8 shows a sequence of SST spatial maps for the months January–June 1989. Note how the initially strong La Niña event dissipates by June 1989.

R tip: Multiple time-indexed spatial maps can be plotted from one long-format table using the functions `facet_grid` or `facet_wrap` in **ggplot2** with time as a grouping variable.

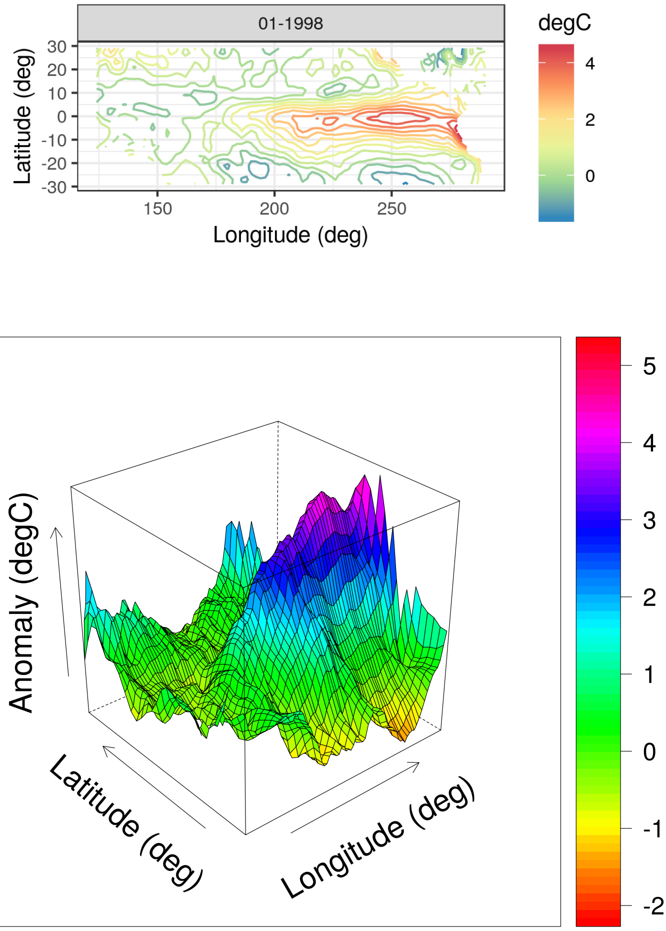

Figure 2.7: Sea-surface temperature anomalies (in °C) for January 1998 as a contour plot (top) and as a surface plot (bottom).

2.3.2 Time-Series Plots

It can be instructive to plot time series corresponding to an observation location, an aggregation of observations, or multiple locations simultaneously. For example, Figure 2.9 shows time-series plots of daily `Tmax` for 10 of the NOAA stations (chosen randomly from the 139 stations) for the time period 01 May 1993–30 September 1993. The time-series plots are quite noisy, as is to be expected from the variability inherent in mid-latitude weather systems. However, there is an overall temporal trend corresponding to the annual seasonal

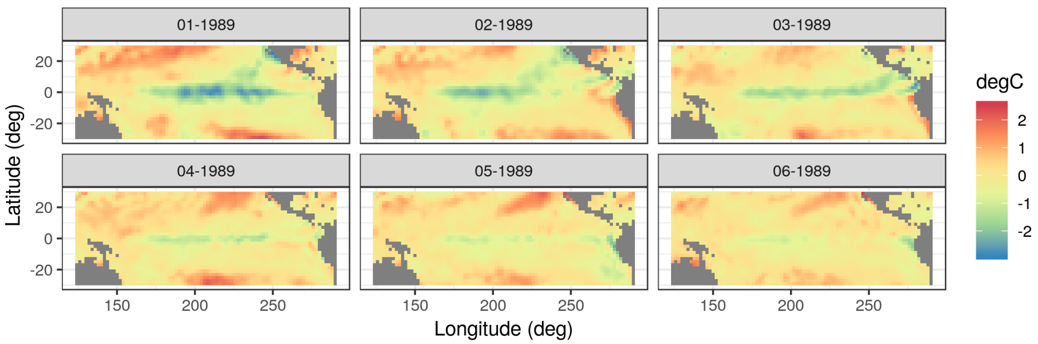

Figure 2.8: Sea-surface temperature anomalies (in °C) for January–June 1989.

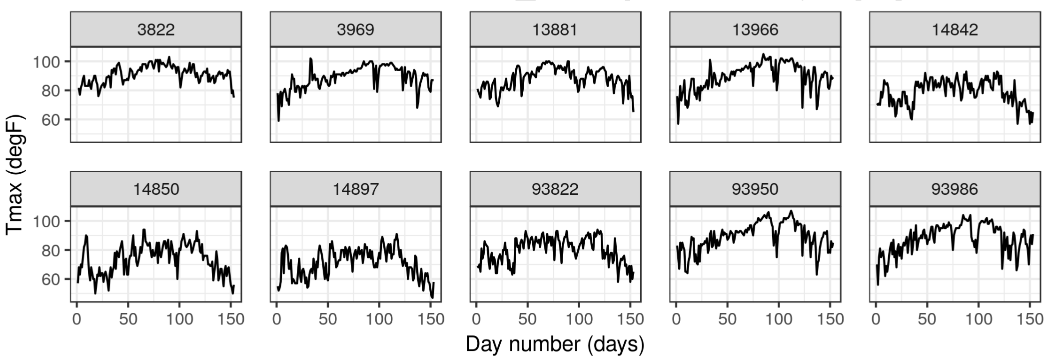

Figure 2.9: Maximum temperature (°F) for ten stations chosen from the NOAA data set at random, as a function of the day number, with the first day denoting 01 May 1993 and the last day denoting 30 September 1993. The number in the grey heading of each plot denotes the station ID.

cycle. That is, all of the time series appear to peak somewhat towards the center of the time horizon, which corresponds to the month of July. In this case, since we are using only five months of data, this trend appears to be roughly quadratic in time. Periodic functions are often used when considering a whole year or multiple years of data, especially with weather and economic data. Although all of these temperature series contain a seasonal component, some appear shifted on the vertical axis (`Tmax`) relative to one another (e.g., station 13881 has higher temperatures than station 14897). This is due to the latitudinal trend apparent in Figure 2.1.

2.3.3 Hovmöller Plots

A Hovmöller plot (Hovmöller, 1949) is a two-dimensional space-time visualization in which space is collapsed (projected or averaged) onto one dimension and where the second dimension denotes time. These plots have traditionally been considered in the atmospheric-science and ocean-science communities to visualize propagating features. For example, the left panel of Figure 2.10 shows monthly SST anomalies averaged from 1°S–1°N and plotted such that longitude (over the Pacific Ocean) is on the x-axis and time (from 1996 to 2003) is on the y-axis (increasing from top to bottom). The darker red colors correspond to warmer than normal temperatures (i.e., El Niño events) and the darker blue colors correspond to colder than normal temperatures (i.e., La Niña events). Propagation through time is evident if a coherent color feature is "slanted." In this plot, one can see several cases of propagating features along the longitudinal axis (e.g., both of the major La Niña events show propagation from the eastern longitudes towards the western longitudes.)

Hovmöller plots are straightforward to generate with regular spatio-temporal data, but they can also be generated for irregular spatio-temporal data after suitable interpolation to a regular space-time grid. For example, in Figure 2.11, we show Hovmöller plots for the `Tmax` variable in the NOAA data set between 01 May 1993 and 30 September 1993. We see that the temporal trend is fairly constant with *longitude* (left panel), but it decreases considerably with increasing *latitude* (right panel) as expected, since overall maximum temperature decreases with increasing latitude in the conterminous USA. Such displays may affect modeling decisions of the trend (e.g., a time–latitude interaction might become evident in such plots).

2.3.4 Interactive Plots

Programming tools for interactive visualization are becoming increasingly accessible. These tools typically allow for a more data-immersive experience, and they allow one to explore the data without having to resort to scripting. In the simplest of cases, one can "hover" a cursor over a figure, and some information related to the data corresponding to the current location of the cursor is conveyed to the user. For example, in Figure 2.12 we show the interaction of the user with a spatial plot of SST using the package **plotly**. This package works in combination with a web portal for more advanced exploration methods (e.g., the exploration of three-dimensional data).

There are several interactive plots that may aid with the visualization of spatio-temporal data. One of the most useful plots builds on *linked brushing*, with the link acting between time and space. Here, one hovers a cursor over a spatial observation or highlights a spatial area, and then the time series corresponding to that point or area is visualized; see Figure 2.12. This allows one to explore the time series corresponding to known geographic areas with minimal effort. Code for generating a linked brush is available from the book's website (`https://spacetimewithr.org`).

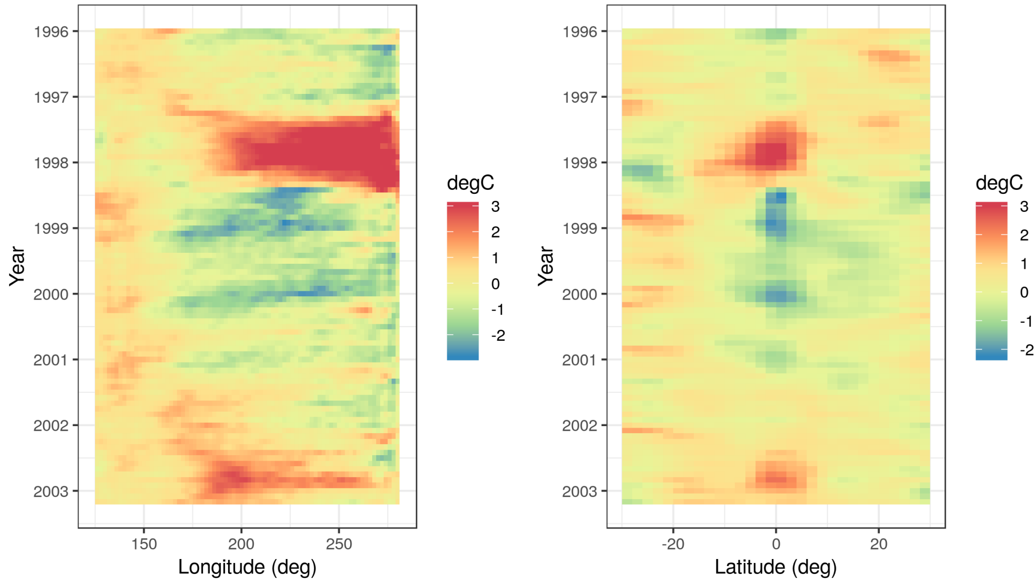

Figure 2.10: Hovmöller plots for both the longitude (left) and latitude (right) coordinates for the SST data set. The color denotes the temperature anomaly in °C.

2.3.5 Animations

Everyone loves a movie. Animation captures our attention and can suggest structure in a way that a sequence of still frames cannot. Good movies should be watched again and again, and that is our intention here for understanding why the spatio-temporal data behave the way they do.

An animation is typically constructed by plotting spatial data frame-by-frame, and then stringing them together in sequence. When doing so, it is important to ensure that all spatial axes and color scales remain constant across all frames. In situations with missing or unequally spaced observations, one may sometimes improve the utility of an animation by performing a simple interpolation (in space and/or time) before constructing the sequence. Animations in `R` can be conveniently produced using the package **animation**. We provide an example using this package in Lab 2.2.

2.3.6 Trelliscope: Visualizing Large Spatio-Temporal Data Sets

Most spatio-temporal statistical analyses to date have been carried out on manageable data sets that can fit into a computer's memory which, at the time of writing, was in the order of a few tens or a couple of hundreds of gigabytes in size. Being able to visualize these data is important and useful in many respects. Proceeding with modeling and prediction where not all the data can be processed in a single place (known as parallel-data algorithms) is an

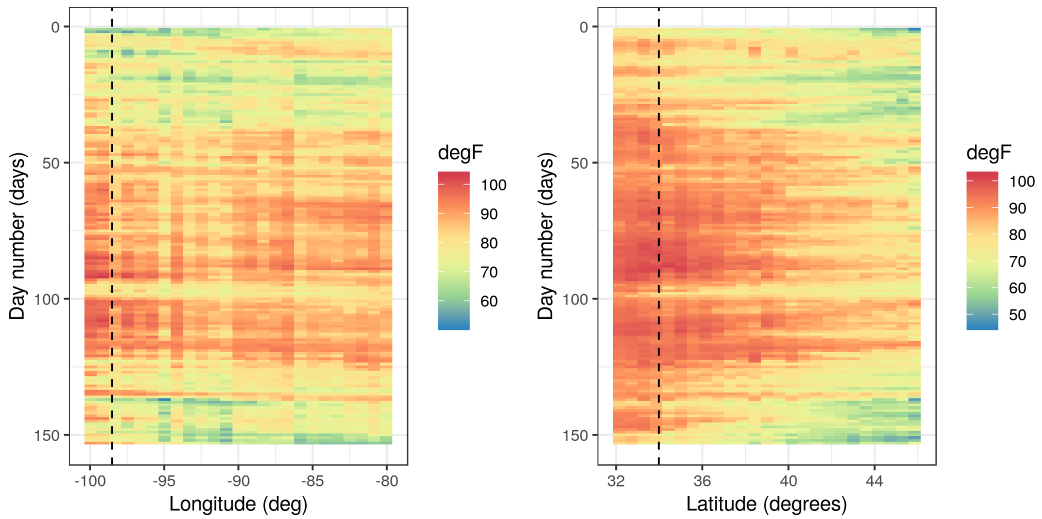

Figure 2.11: Hovmöller plots for both the longitude (left) and latitude (right) coordinates for the `Tmax` variable in the NOAA data set between 01 May 1993 and 30 September 1993, where the data are interpolated as described in Lab 2.2. The color denotes the maximum temperature in °F. The dashed lines correspond to the longitude and latitude coordinates of station 13966 (compare to Figure 2.9).

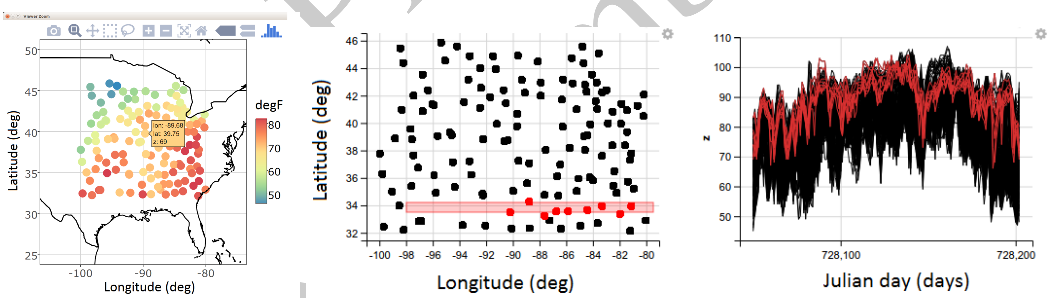

Figure 2.12: Interactively exploring maximum temperatures on 01 May 1993 using the NOAA data set. The "hover" feature can be added to **ggplot2** objects by using `ggplotly` from the package **plotly** (left). A linked brush can be used to explore the time series (right) corresponding to a user-chosen set of spatial locations (middle) with the package **ggvis**.

active area of research and will not be discussed here.

The Trelliscope system, available with the package **trelliscope**, helps users visualize massive data sets. The first advantage of **trelliscope** is that it facilitates exploration when, due to its size, the data may only be visualized using hundreds or thousands of plots (or panels). When this is the case, the Trelliscope system can calculate subset summaries (known as *cognostics*) that are then used for filtering and sorting the panels. For example, consider the SST data set. If a grouping is made by month, then there are over 300 spatial maps that can be visualized between, say, 1970 and 2003. Alternatively, one may decide to visualize only those months in which the SST exceeded a certain maximum or minimum threshold. One can formulate a cognostic using the monthly spatial mean values of SST averaged over their spatial domain and visualize them in a quantile plot (see Figure 2.13). The analyst can use this approach to quickly view the strongest El Niño and La Niña events in this time period.

The second advantage is that the **trelliscope** package is designed to visualize data that are on a distributed file system that may be residing on more than one node. The data are processed in a *divide and recombine* fashion; that is, the data are divided and processed by group in parallel fashion and then recombined. In **trelliscope**, this can be useful for generating both the cognostics and the viewing panels efficiently. Therefore, the Trelliscope system provides a way to visualize terabytes of space-time data but, as quoted in its package manual, it "can also be very useful for small data sets."

R tip: Processing and visualizing large data sets residing on a distributed file system using divide and recombine may seem like a daunting task. The R package **datadr**, which can be used together with **trelliscope**, provides an easy-to-use front-end for data residing on distributed file systems. More importantly, it reduces the barrier to entry by allowing the same, or very similar, code to be used for data residing in memory and data residing on a distributed file system such as Hadoop.

2.3.7 Visualizing Uncertainty

One of the main things that separates statistics from other areas of data science is the focus on uncertainty quantification. Uncertainties could be associated with data (e.g., measurement error in satellite observations or sampling error in a survey), estimates (e.g., uncertainty in regression parameter estimates), or predictions (e.g., uncertainties in a forecast of SST anomalies). Taking a Bayesian point of view, uncertainties could also be associated with the parameters themselves. In the case where these uncertainties are indexed in time, space, or space-time, one can use any of the methods discussed in this section to produce visualizations of these uncertainties. It is increasingly the case that one seeks methods to visualize both the values of interest and their uncertainty simultaneously. This is challenging given the difficulties in visualizing information in multiple dimensions, and it is an active area of research both in geography and statistics (see, for example, the discussion of "visuanimation" in Genton et al., 2015). For a recent overview in the case of areal data, and

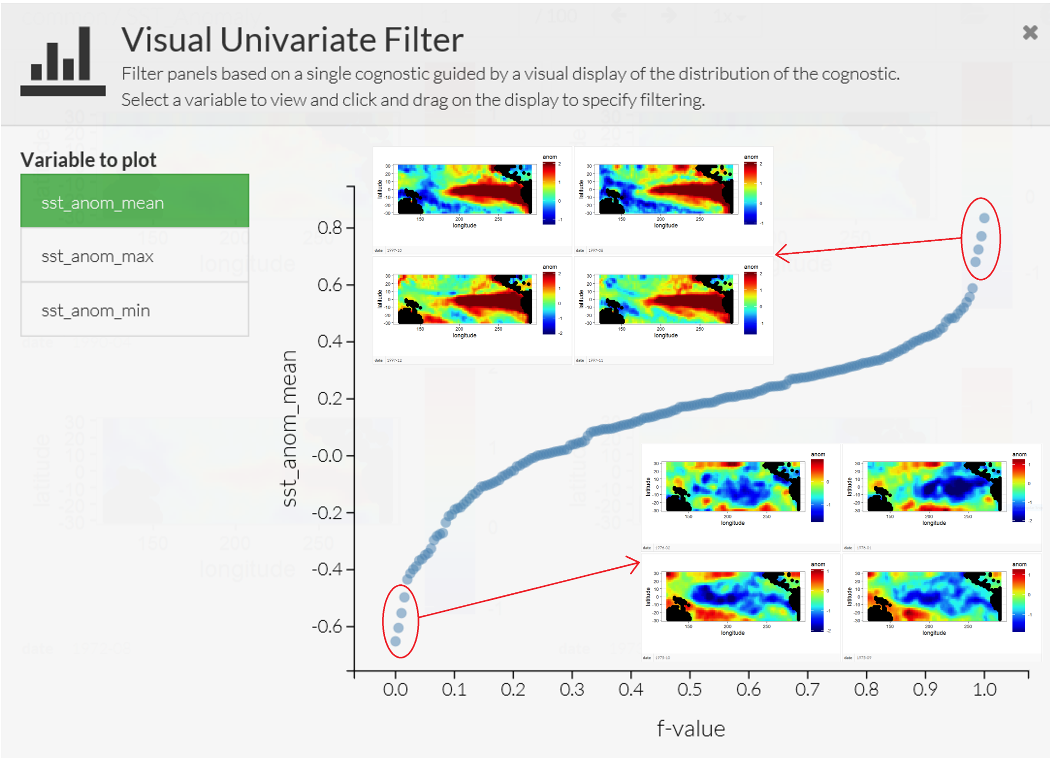

Figure 2.13: Exploring a large spatio-temporal data set with Trelliscope. Quantile plot of monthly averages of sea-surface temperature from the SST data set; the insets are what would be displayed if the user highlighted the circle points, corresponding to El Niño and La Niña events.

an accompanying R vignette, see Lucchesi and Wikle (2017) and the R package **Vizumap**.[5]

2.4 Exploratory Analysis of Spatio-Temporal Data

Visualization of data is certainly an important and necessary component of exploratory data analysis. In addition, we often wish to explore spatio-temporal data in terms of summaries of first-order and second-order characteristics. Here we consider visualizations of empirical means and empirical covariances, spatio-temporal covariograms and semivariograms, the use of empirical orthogonal functions and their associated principal-component time series, and spatio-temporal canonical correlation analysis. To do this, we have to start using some mathematical symbols and formulas. Mathematics is the language of science (and of statistical science), and we introduce this language along the way to help readers who are a

[5] `https://doi.org/10.5281/zenodo.1479951`

bit less fluent. For reference, we present some fundamental definitions of vectors and matrices and their manipulation in Appendix A. Readers who are not familiar with the symbols and basic manipulation of vectors and matrices would benefit from looking at this material before proceeding.

2.4.1 Empirical Spatial Means and Covariances

It can be useful to explore spatio-temporal data by examining the empirical means and empirical covariances. Assume for the moment that we have observations $\{Z(\mathbf{s}_i;t_j)\}$ for spatial locations $\{\mathbf{s}_i : i = 1,\ldots,m\}$ and times $\{t_j : j = 1,\ldots,T\}$. The empirical spatial mean for location $\mathbf{s}_i$, $\widehat{\mu}_{z,s}(\mathbf{s}_i)$, is then found by averaging over time:

$$\widehat{\mu}_{z,s}(\mathbf{s}_i) \equiv \frac{1}{T}\sum_{j=1}^{T} Z(\mathbf{s}_i;t_j).$$

If we consider the means for all spatial data locations and assume that we have T observations at each location, then we can write down the spatial mean as an m-dimensional vector, $\widehat{\boldsymbol{\mu}}_{z,s}$, where

$$\widehat{\boldsymbol{\mu}}_{z,s} \equiv \begin{bmatrix} \widehat{\mu}_{z,s}(\mathbf{s}_1) \\ \vdots \\ \widehat{\mu}_{z,s}(\mathbf{s}_m) \end{bmatrix} = \begin{bmatrix} \frac{1}{T}\sum_{j=1}^{T} Z(\mathbf{s}_1;t_j) \\ \vdots \\ \frac{1}{T}\sum_{j=1}^{T} Z(\mathbf{s}_m;t_j) \end{bmatrix} = \frac{1}{T}\sum_{j=1}^{T}\mathbf{Z}_{t_j}, \tag{2.1}$$

and $\mathbf{Z}_{t_j} \equiv (Z(\mathbf{s}_1;t_j),\ldots,Z(\mathbf{s}_m;t_j))'$.

This mean vector is a spatial quantity whose elements are indexed by their location. Therefore, it can be plotted on a map, as in the case of the maximum temperature in the NOAA data set (see Figure 2.1), or as a function of the spatial coordinates (e.g., longitude or latitude) as in Figure 2.14. From these plots one can see that there is a clear trend in the empirical spatial mean of maximum temperature with latitude, but not so much with longitude. Note that one may not have the same number of observations at each location to calculate the average, in which case each location in space must be calculated separately (e.g., $\widehat{\mu}_{z,s}(\mathbf{s}_i) = (1/T_i)\sum_{j=1}^{T_i} Z(\mathbf{s}_i;t_j)$, where T_i is the number of time points at which there are data at location $\mathbf{s}_i$).

Additionally, one can average across space and plot the associated time series. The empirical temporal mean for time t_j, $\widehat{\mu}_{z,t}(t_j)$, is given by

$$\widehat{\mu}_{z,t}(t_j) \equiv \frac{1}{m}\sum_{i=1}^{m} Z(\mathbf{s}_i;t_j). \tag{2.2}$$

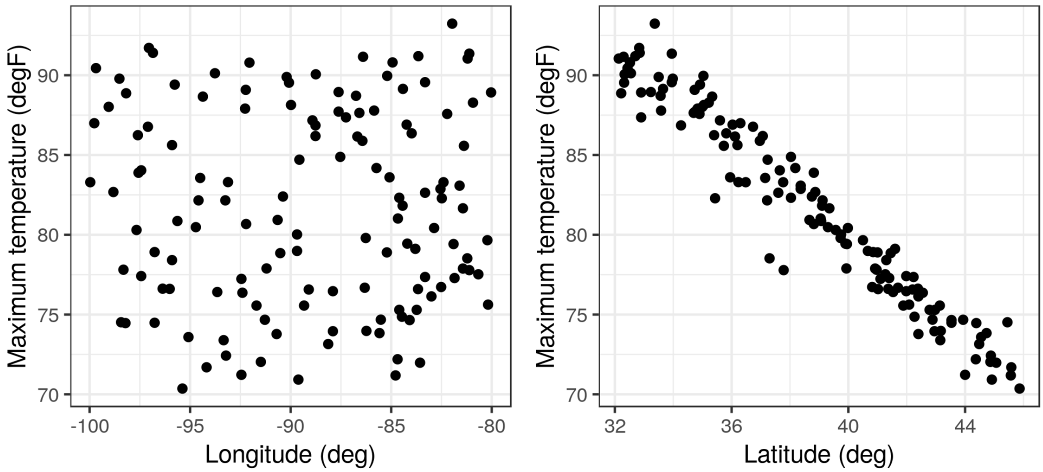

Figure 2.14: Empirical spatial mean, $\widehat{\mu}_{z,s}(\cdot)$, of `Tmax` (in °F) as a function of station longitude (left) and station latitude (right).

For example, Figure 2.15 shows the time series of `Tmax` for the NOAA temperature data set averaged across all of the spatial locations. This plot of the empirical temporal means shows the seasonal nature of the mid-latitude temperature over the central USA, but it also shows variations in that seasonal pattern due to specific large-scale weather systems.

> **R tip:** Computing empirical means is quick and easy using functions in the package **dplyr**. For example, to find a temporal average, the data in a long-format data frame can first be grouped by spatial location using the function `group_by`. A mean can then be computed for every spatial location using the function `summarise`. See Lab 2.1 for more details on these functions.

It is often useful to consider the empirical spatial covariability in the spatio-temporal data set. This covariability can be used to determine to what extent data points in the data set covary (behave similarly) as a function of space and/or time. In the context of the data described above, the empirical lag-τ covariance between spatial locations $\mathbf{s}_i$ and $\mathbf{s}_k$ is given by

$$\widehat{C}_z^{(\tau)}(\mathbf{s}_i, \mathbf{s}_k) \equiv \frac{1}{T-\tau} \sum_{j=\tau+1}^{T} (Z(\mathbf{s}_i; t_j) - \widehat{\mu}_{z,s}(\mathbf{s}_i))(Z(\mathbf{s}_k; t_j - \tau) - \widehat{\mu}_{z,s}(\mathbf{s}_k)), \qquad (2.3)$$

for $\tau = 0, 1, \ldots, T-1$, which is called the empirical lag-τ spatial covariance. Note that this is the average (over time) of the cross products of the centered observations at the two

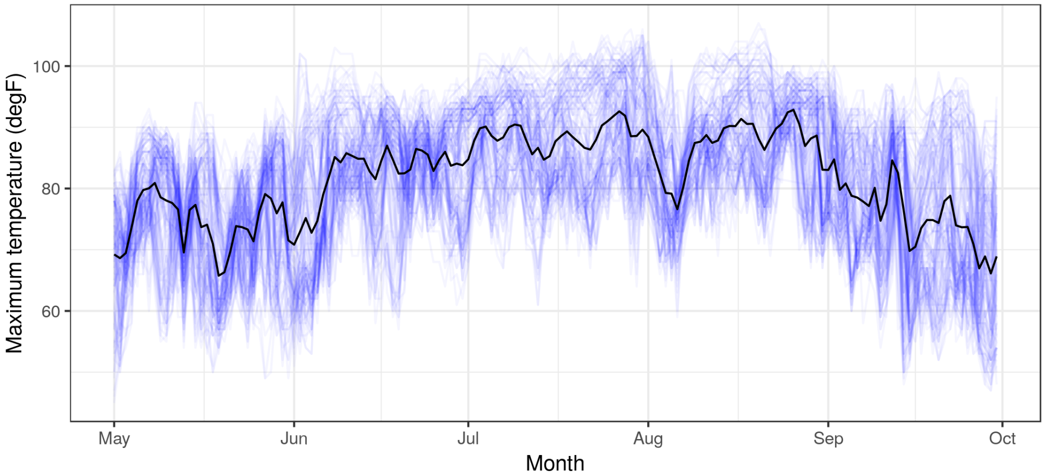

Figure 2.15: `Tmax` data (in °F), from the NOAA data set (blue lines, where each blue line corresponds to a station) and the empirical temporal mean $\widehat{\mu}_{z,t}(\cdot)$ (black line) computed from (2.2), and t is in units of days, ranging from 01 May 1993 to 30 September 1993.

locations ($\mathbf{s}_i$ and $\mathbf{s}_k$); that is, (2.3) is a summary of the covariation of these data. It is often useful to consider the $m \times m$ lag-τ empirical spatial covariance matrix, $\widehat{\mathbf{C}}_z^{(\tau)}$, in which the (i, k)th element is given by (2.3). Alternatively, this can be calculated directly by

$$\widehat{\mathbf{C}}_z^{(\tau)} \equiv \frac{1}{T-\tau} \sum_{j=\tau+1}^{T} (\mathbf{Z}_{t_j} - \widehat{\boldsymbol{\mu}}_{z,s})(\mathbf{Z}_{t_j-\tau} - \widehat{\boldsymbol{\mu}}_{z,s})'; \quad \tau = 0, 1, \ldots, T-1. \tag{2.4}$$

Thus, in order to find the lag-τ covariance matrices, we consider the cross products of the residual vectors for each spatial location and each time point relative to its corresponding time-averaged empirical spatial mean.

In general, it can be difficult to obtain any intuition from these matrices, since locations in a two-dimensional space do not have a natural ordering. However, one can sometimes gain insight by splitting the domain into "strips" corresponding to one of the spatial dimensions (e.g., longitudinal strips) and then plotting the associated covariance matrices for those strips. For example, Figure 2.16 shows empirical covariance matrices for the maximum temperature in the NOAA data set (after, as shown in Lab 2.3, a quadratic trend in time has been removed), split into four longitudinal strips. Not surprisingly, these empirical spatial covariance matrices reveal the presence of spatial dependence in the residuals. The lag-0 plots seem to be qualitatively similar, suggesting that there is no strong correlational dependence on longitude but that there is a correlational dependence on latitude, with the spatial covariance decreasing with decreasing latitude.

We can also calculate the empirical lag-τ cross-covariance matrix between two spatio-temporal data sets, $\{\mathbf{Z}_{t_j}\}$ and $\{\mathbf{X}_{t_j}\}$, where $\{\mathbf{X}_{t_j}\}$ corresponds to data vectors at n different locations (but it is assumed for meaningful comparisons that they correspond to the same time points). In particular, we define this $m \times n$ matrix by

$$\widehat{\mathbf{C}}_{z,x}^{(\tau)} \equiv \frac{1}{T-\tau} \sum_{j=\tau+1}^{T} (\mathbf{Z}_{t_j} - \widehat{\boldsymbol{\mu}}_{z,s})(\mathbf{X}_{t_j-\tau} - \widehat{\boldsymbol{\mu}}_{x,s})', \tag{2.5}$$

for $\tau = 0, 1, \ldots, T-1$, where $\widehat{\boldsymbol{\mu}}_{x,s}$ is the empirical spatial mean vector for the data $\{\mathbf{X}_{t_j}\}$. Cross-covariances may be useful in characterizing the spatio-temporal dependence relationship between two different variables, for example maximum temperature and minimum temperature.

Although not as common in spatio-temporal applications, one can also calculate empirical temporal covariance matrices averaging across space (after *removing temporal means* averaged across space). In this case, the time index is unidimensional and ordered, so one does not have to work as hard on the interpretation as we did with empirical spatial covariance matrices.

2.4.2 Spatio-Temporal Covariograms and Semivariograms

In Chapter 4 we shall see that it is necessary to characterize the joint spatio-temporal dependence structure of a spatio-temporal process in order to perform optimal prediction (i.e., kriging). Thus, for measures of the joint spatio-temporal dependence, we consider empirical spatio-temporal *covariograms* (and their close cousins, *semivariograms*). The biggest difference between what we are doing here and the covariance estimates in the previous section is that we are interested in characterizing the covariability in the spatio-temporal data as a function of specific lags in time *and* in space. Note that the lag in time is a scalar, but the lag in space is a vector (corresponding to the displacement between locations in d-dimensional space).

Consider the empirical spatio-temporal covariance function for various space and time lags. Here, we make an assumption that the first moment (mean) depends on space but not on time and that the second moment (covariance) depends only on the lag differences in space and time. Then the empirical spatio-temporal covariogram for spatial lag $\mathbf{h}$ and time lag τ is given by

$$\widehat{C}_z(\mathbf{h};\tau) = \frac{1}{|N_{\mathbf{s}}(\mathbf{h})|}\frac{1}{|N_t(\tau)|} \sum_{\mathbf{s}_i,\mathbf{s}_k \in N_{\mathbf{s}}(\mathbf{h})} \sum_{t_j,t_\ell \in N_t(\tau)} (Z(\mathbf{s}_i;t_j) - \widehat{\mu}_{z,s}(\mathbf{s}_i))(Z(\mathbf{s}_k;t_\ell) - \widehat{\mu}_{z,s}(\mathbf{s}_k)), \tag{2.6}$$

where you will recall that $\widehat{\mu}_{z,s}(\mathbf{s}_i) = (1/T)\sum_{j=1}^{T} Z(\mathbf{s}_i;t_j)$, $N_{\mathbf{s}}(\mathbf{h})$ refers to the pairs of spatial locations with spatial lag within some tolerance of $\mathbf{h}$, $N_t(\tau)$ refers to the pairs of time points with time lag within some tolerance of τ, and $|N(\cdot)|$ refers to the number of elements in $N(\cdot)$. Under *isotropy*, one often considers the lag only as a function of distance, $h = ||\mathbf{h}||$, where $||\cdot||$ is the Euclidean norm (see Appendix A).

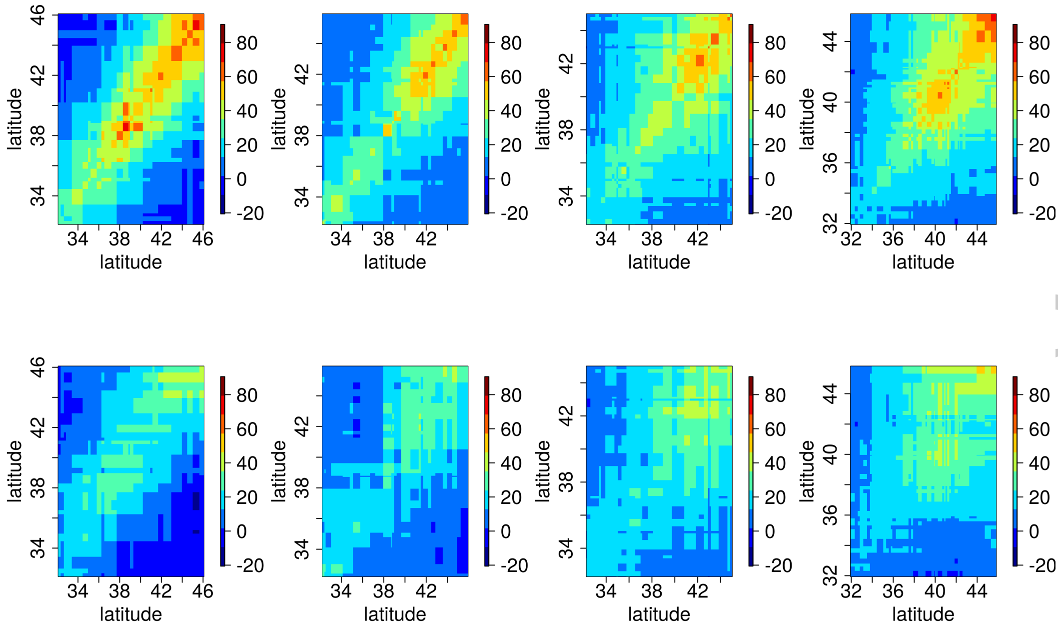

Figure 2.16: Maximum temperature lag-0 (top) and lag-1 (bottom) empirical spatial covariance plots for four longitudinal strips (from left to right, $[-100, -95), [-95, -90), [-90, -85), [-85, -80)$ degrees) in which the domain of interest is subdivided.

Technical Note 2.1: Semivariogram

The semivariogram is defined as

$$\gamma_z(\mathbf{s}_i, \mathbf{s}_k; t_j, t_\ell) \equiv \frac{1}{2}\mathrm{var}(Z(\mathbf{s}_i; t_j) - Z(\mathbf{s}_k; t_\ell)).$$

In the case where the covariance depends only on displacements in space and differences in time, this can be written as

$$\begin{aligned} \gamma_z(\mathbf{h}; \tau) &= \frac{1}{2}\mathrm{var}(Z(\mathbf{s} + \mathbf{h}; t + \tau) - Z(\mathbf{s}; t)) \\ &= C_z(\mathbf{0}; 0) - \mathrm{cov}(Z(\mathbf{s} + \mathbf{h}; t + \tau), Z(\mathbf{s}; t)) \\ &= C_z(\mathbf{0}; 0) - C_z(\mathbf{h}; \tau), \end{aligned} \tag{2.7}$$

where $\mathbf{h} = \mathbf{s}_k - \mathbf{s}_i$ is a spatial lag and $\tau = t_\ell - t_j$ is a temporal lag.

Now, (2.7) does not always hold. It is possible that γ_z is a function of spatial lag $\mathbf{h}$ and temporal lag τ, but there is no stationary covariance function $C_z(\mathbf{h}; \tau)$. We generally try to avoid these models of covariability by fitting trend terms that are linear and/or quadratic in spatio-temporal coordinates.

If the covariance function of the process is well defined, then the semivariogram is generally characterized by the nugget effect, the sill, and the partial sill. The nugget effect is given by $\gamma_z(\mathbf{h};\tau)$ when $\mathbf{h} \to \mathbf{0}$ and $\tau \to 0$, while the sill is $\gamma_z(\mathbf{h};\tau)$ when $\mathbf{h} \to \infty$ and $\tau \to \infty$. The partial sill is the difference between the sill and the nugget effect. The diagram below shows these components of a semivariogram as a function of spatial distance $\|\mathbf{h}\|$.

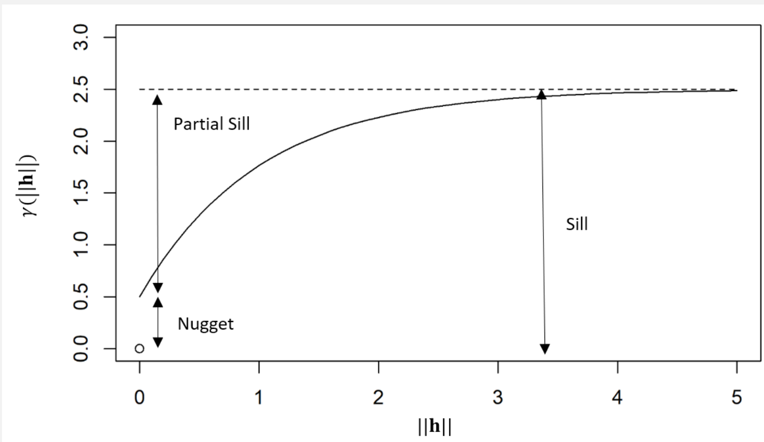

In some kriging applications, one might be interested in looking at the empirical spatio-temporal semivariogram (see Technical Note 2.1). The empirical semivariogram, for the case where the covariance only depends on the displacements in space and the time lags, is obtained from (2.6) as $\widehat{\gamma}_z(\mathbf{h};\tau) = \widehat{C}_z(\mathbf{0};0) - \widehat{C}_z(\mathbf{h};\tau)$, and so it is easy to go back and forth between the empirical semivariogram and the covariogram in this case (see the caveat in Technical Note 2.1). Assuming a constant spatial mean $\mu_{z,s}$, then (2.7) can be equivalently written as

$$\gamma_z(\mathbf{h};\tau) = \frac{1}{2} E\left(Z(\mathbf{s}+\mathbf{h};t+\tau) - Z(\mathbf{s};t)\right)^2,$$

and hence an alternative estimate is

$$\widehat{\gamma}_z(\mathbf{h};\tau) = \frac{1}{|N_{\mathbf{s}}(\mathbf{h})|}\frac{1}{|N_t(\tau)|} \sum_{\mathbf{s}_i,\mathbf{s}_k \in N_{\mathbf{s}}(\mathbf{h})} \sum_{t_j,t_\ell \in N_t(\tau)} (Z(\mathbf{s}_i;t_j) - Z(\mathbf{s}_k;t_\ell))^2, \tag{2.8}$$

where the notation in (2.8) is the same as used above in (2.6). Note that this calculation does not need any information about the spatial means. Figure 2.17 shows a semivariogram obtained from the NOAA data set for the maximum temperature data in July 1993.

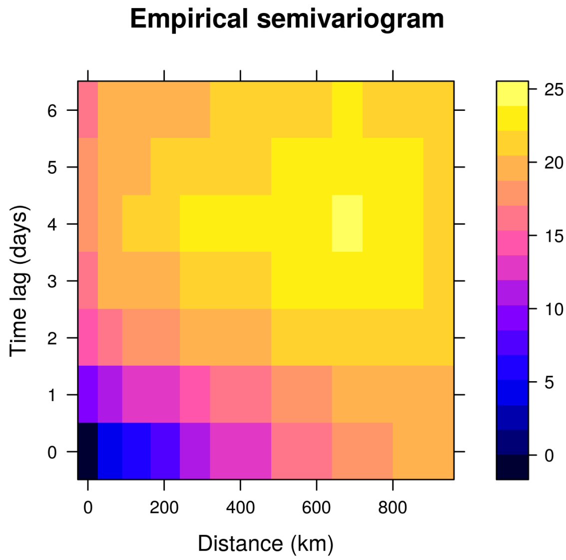

Figure 2.17: Empirical spatio-temporal semivariogram of daily `Tmax` from the NOAA data set during July 2003, computed using the function **`variogram`** in **gstat**.

2.4.3 Empirical Orthogonal Functions (EOFs)

Empirical orthogonal functions (EOFs) can reveal spatial structure in spatio-temporal data and can also be used for subsequent dimensionality reduction. EOFs came out of the meteorology/climatology literature, and in the context of discrete space and time, EOF analysis is the spatio-temporal manifestation of principal component analysis (PCA) in statistics (see Chapter 5 in Cressie and Wikle, 2011, for an extensive overview). In the terminology of this chapter, one should probably modify "EOFs" to empirical *spatial* orthogonal functions, since they are obtained from an empirical *spatial* covariance matrix, but for legacy reasons we stick with "EOFs." Before we discuss EOFs, we give a brief review of PCA.

Brief Review of Principal Component Analysis

Assume we have two measured traits on a subject of interest (e.g., measurements of $x_1 =$ height (in cm) and $x_2 =$ weight (in kg) in a sample of women in the USA). Figure 2.18 (left panel) shows a (simulated) plot of what such data might look like for $m = 500$ individuals. We note that these data are quite correlated, as expected. Now, we wish to construct new variables that are linear combinations of the measured traits, say $a_1 = w_{11}x_1 + w_{12}x_2$ and $a_2 = w_{21}x_1 + w_{22}x_2$. One way to think of this is that we are "projecting" the original data onto new axes given by the variables a_1 and a_2. Figure 2.18 (center and right panels) shows

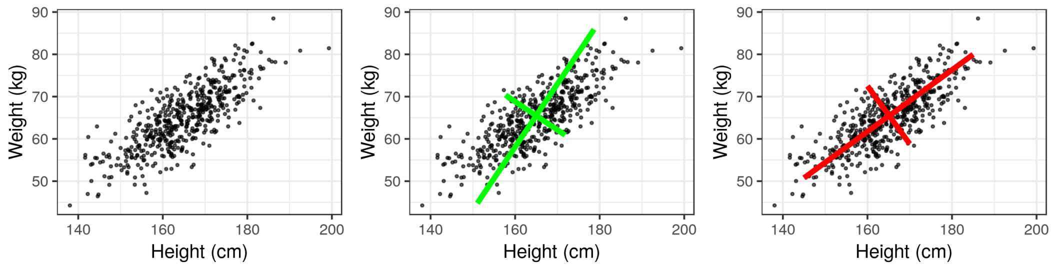

Figure 2.18: Simulated height (in cm) versus weight (in kg) for $m = 500$ females in the USA (left) with two orthogonal projections (center and right). The right panel shows the optimal PCA projection.

two possible projections, which differ according to the values we choose for the weights, $\{w_{11}, w_{12}, w_{21}, w_{22}\}$. Note that in the case of the right-hand panel in Figure 2.18, the new axis a_1 aligns with the axis of largest variation, and the new axis a_2 corresponds to the axis of largest variation perpendicular (orthogonal) to the axis a_1. Maximizing these axes of variation subject to orthogonality helps us think about decomposing the data into lower-dimensional representations in an optimal way. That is, the new variable on the axis a_1 represents the optimal linear combination of the data that accounts for the most variation in the original data. If the variation along the other axis (a_2) is fairly small relative to a_1, then it might be sufficient just to consider a_1 to represent the data.

How does one go about choosing the weights $\{w_{ij}\}$? Let $\mathbf{x}_i = (x_{1i}, \ldots, x_{pi})'$ be a random vector with variance–covariance matrix $\mathbf{C}_x$. Note from Appendix A that by spectral decomposition, a $p \times p$ non-negative-definite, symmetric, real matrix, $\boldsymbol{\Sigma}$, can be *diagonalized* such that $\mathbf{W}'\boldsymbol{\Sigma}\mathbf{W} = \boldsymbol{\Lambda}$ (i.e., $\boldsymbol{\Sigma} = \mathbf{W}\boldsymbol{\Lambda}\mathbf{W}'$), where $\boldsymbol{\Lambda}$ is a diagonal matrix containing the eigenvalues $\{\lambda_i\}$ of $\boldsymbol{\Sigma}$ (where $\lambda_1 \geq \lambda_2 \geq \ldots \geq \lambda_p \geq 0$) and $\mathbf{W} = [\mathbf{w}_1 \; \mathbf{w}_2 \; \ldots \; \mathbf{w}_p]$ is the associated matrix of orthogonal eigenvectors, $\{\mathbf{w}_i\}$ (i.e., $\mathbf{W}\mathbf{W}' = \mathbf{W}'\mathbf{W} = \mathbf{I}$); thus, $\mathbf{C}_x = \mathbf{W}\boldsymbol{\Lambda}_x\mathbf{W}'$. It can be shown that these eigenvectors give the optimal weights, so that $\mathbf{w}_1$ are the weights for a_1 and $\mathbf{w}_2$ are the weights for a_2, and so on.

As an example, consider the variance–covariance matrix associated with the simulated height and weight traits, where $p = 2$:

$$\mathbf{C}_x = \begin{pmatrix} 81 & 50 \\ 50 & 49 \end{pmatrix}.$$

Then $\mathbf{W}$ and $\boldsymbol{\Lambda}_x$ are given (using the function `eigen` in R) by

$$\mathbf{W} = \begin{pmatrix} -0.8077 & 0.5896 \\ -0.5896 & -0.8077 \end{pmatrix}, \quad \boldsymbol{\Lambda}_x = \begin{pmatrix} 117.5 & 0 \\ 0 & 12.5 \end{pmatrix}.$$

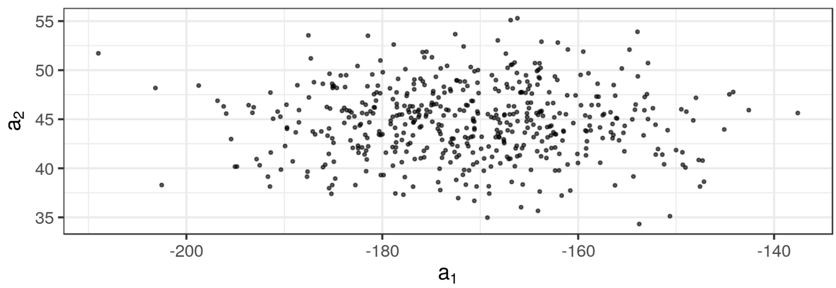

Figure 2.19: Principal components corresponding to the simulated data in Figure 2.18.

So, for each of the observation vectors, $\{\mathbf{x}_i, i = 1, \ldots, 500\}$, we make new variables

$$a_{1i} = -0.8077x_{1i} - 0.5896x_{2i}$$

$$a_{2i} = 0.5896x_{1i} - 0.8077x_{2i}.$$

These coefficients (which are the data projected onto axes (a_1, a_2)) are plotted in Figure 2.19. Note that these new variables are uncorrelated (no slant to the points in the plot) and the first axis (a_1) corresponds to the one that has the most variability. In PCA, one sometimes attempts to interpret the "loadings" given by $\{\mathbf{w}_i : i = 1, \ldots, p\}$ (or some scaled version of them). That is, one contrasts the signs and magnitudes of the loadings within a given eigenvector (e.g., the first eigenvector, $\mathbf{w}_1 = (-0.8077, -0.5896)'$, suggests that both height and weight are important and vary in the same way, so that the first principal component might represent an overall "size" attribute).

The notions presented in the example above extend to more than just two traits and, in general, the principal-component decomposition has some nice properties. For example, the kth eigenvalue is the variance of the associated linear combination of the elements of $\mathbf{x}$; that is, $\text{var}(a_k) = \text{var}(\mathbf{w}_k'\mathbf{x}) = \lambda_k$. In addition,

$$\text{var}(x_1) + \ldots \text{var}(x_p) = \text{trace}(\mathbf{C}_x) = \lambda_1 + \ldots + \lambda_p = \text{var}(a_1) + \ldots + \text{var}(a_p).$$

Thus, one can consider the proportion of the total variance accounted for by the kth principal component, which is $\lambda_k / \sum_{j=1}^{p} \lambda_j$. In the example above, the first principal component accounts for about 90% of the variance in the original data (i.e., $\lambda_1/(\lambda_1 + \lambda_2) = 117.5/130 = 0.90$).

Of course, in practice we would not know the covariance matrix, $\mathbf{C}_x$, but we can calculate an empirical covariance matrix using (2.4) with $\tau = 0$, $\{\mathbf{Z}_{t_j}\}$ replaced by $\{\mathbf{x}_i\}$, and $\widehat{\boldsymbol{\mu}}_{z,s}$ replaced by $(1/500)\sum_{i=1}^{500} \mathbf{x}_i$. In that case, the spectral decomposition of $\widehat{\mathbf{C}}_x$ gives empirical estimates of the eigenvectors $\widehat{\mathbf{W}}$ and eigenvalues $\widehat{\mathbf{\Lambda}}_x$. The analysis then proceeds with these empirical estimates.

R tip: The PCA routine `prcomp` is included with base R. When the `plot` function is used on an object returned by `prcomp`, the variances of the principal components are displayed. The function `biplot` returns a plot showing how the observations relate to the principal components.

Empirical Orthogonal Functions

The study of EOFs is related to PCA in the sense that the "traits" of the multivariate data vector now are spatially indexed, and the samples are usually taken over time. It is shown in Cressie and Wikle (2011, Chapter 5) that the EOFs can be obtained from the data through either a spectral decomposition of an empirical (spatial or temporal) covariance matrix or a singular value decomposition (SVD) of a centered data matrix (see Technical Note 2.2).

Let $\mathbf{Z}_{t_j} \equiv (Z(\mathbf{s}_1; t_j), \ldots, Z(\mathbf{s}_m; t_j))'$ for $j = 1, \ldots, T$. Using (2.4) to estimate the lag-0 spatial covariance matrix, $\widehat{\mathbf{C}}_z^{(0)}$ (which is symmetric and non-negative-definite), the PCA decomposition is given by the spectral decomposition

$$\widehat{\mathbf{C}}_z^{(0)} = \mathbf{\Psi}\mathbf{\Lambda}\mathbf{\Psi}', \tag{2.9}$$

where $\mathbf{\Psi} \equiv (\boldsymbol{\psi}_1, \ldots, \boldsymbol{\psi}_m)$ is a matrix of spatially indexed eigenvectors given by the vectors $\boldsymbol{\psi}_k \equiv (\psi_k(\mathbf{s}_1), \ldots, \psi_k(\mathbf{s}_m))'$ for $k = 1, \ldots, m$, and $\mathbf{\Lambda} \equiv \mathrm{diag}(\lambda_1, \ldots, \lambda_m)$ is a diagonal matrix of corresponding non-negative eigenvalues (decreasing down the diagonal). The eigenvectors are called "EOFs" and are often plotted as spatial maps (since they are spatially indexed, which is also why $\mathbf{\Psi}$ is used to distinguish them from the more general PCA weights, $\mathbf{W}$, above). For $k = 1, \ldots, m$, the so-called *kth principal component (PC) time series* are given by $a_k(t_j) \equiv \boldsymbol{\psi}_k' \mathbf{Z}_{t_j}$, where $j = 1, \ldots, T$. From PCA considerations, the EOFs have the nice property that $\boldsymbol{\psi}_1$ provides the linear coefficients such that $\mathrm{var}(a_1) = \lambda_1$ is maximized, $\boldsymbol{\psi}_2$ provides the linear coefficients such that $\mathrm{var}(a_2) = \lambda_2$ accounts for the next largest variance such that $\mathrm{cov}(a_1, a_2) = 0$, and so on. As with the principal components in PCA, the EOFs form a discrete orthonormal basis (i.e., $\mathbf{\Psi}'\mathbf{\Psi} = \mathbf{\Psi}\mathbf{\Psi}' = \mathbf{I}$).

There are two primary uses for EOFs. First, it is sometimes the case that one can gain some understanding about important spatial patterns of variability in a sequence of spatio-temporal data by examining the EOF coefficient maps (loadings). But care must be taken not to interpret the EOF spatial structures in terms of dynamical or kinematic properties of the underlying process (see, for example, Monahan et al., 2009). Second, these bases can be quite useful for dimension reduction in a random-effects spatial or spatio-temporal representation (see Section 4.4), although again, in general, they are not "optimal" bases in terms of reduced-order dynamical systems.

Technical Note 2.2: Calculating EOFs

As stated above, EOFs can be calculated directly from the spectral decomposition of the empirical lag-0 spatial covariance matrix (2.9). However, they are more often obtained directly through a *singular value decomposition* (SVD, see Appendix A), which provides computational benefits in some situations. To see the equivalence, first we show how to calculate the empirical covariance-based EOFs. Let $\mathbf{Z} \equiv [\mathbf{Z}_1, \ldots, \mathbf{Z}_T]'$ be the $T \times m$ space-wide data matrix and then let $\widetilde{\mathbf{Z}}$ be the "detrended" and scaled data matrix,

$$\widetilde{\mathbf{Z}} \equiv \frac{1}{\sqrt{T-1}}(\mathbf{Z} - \mathbf{1}_T \widehat{\boldsymbol{\mu}}'_{z,s}), \tag{2.10}$$

where $\mathbf{1}_T$ is a T-dimensional vector of ones and $\widehat{\boldsymbol{\mu}}_{z,s}$ is the spatial mean vector given by (2.1). Then it is easy to show that

$$\mathbf{C}_z^{(0)} = \widetilde{\mathbf{Z}}'\widetilde{\mathbf{Z}} = \boldsymbol{\Psi}\boldsymbol{\Lambda}\boldsymbol{\Psi}', \tag{2.11}$$

and the principal component (PC) time series are given by the columns of $\mathbf{A} = (\sqrt{T-1})\widetilde{\mathbf{Z}}\boldsymbol{\Psi}$; that is, they are projections of the detrended data matrix onto the EOF basis functions, $\boldsymbol{\Psi}$. The *normalized PC time series* are then given by $\mathbf{A}_{\mathrm{norm}} \equiv \mathbf{A}\boldsymbol{\Lambda}^{-1/2}$; these are just the PC time series divided by their standard deviation (i.e., the square root of the associated eigenvalue), so that the temporal variance of the normalized time series is equal to one. This normalization allows the m time series to be plotted on the same scale, leaving their relative importance to be captured by their corresponding eigenvalues.

Now, consider the SVD of the detrended and scaled data matrix,

$$\widetilde{\mathbf{Z}} = \mathbf{U}\mathbf{D}\mathbf{V}', \tag{2.12}$$

where $\mathbf{U}$ is the $T \times T$ matrix of left singular vectors, $\mathbf{D}$ is a $T \times m$ matrix containing singular values on the main diagonal, and $\mathbf{V}$ is an $m \times m$ matrix containing the right singular vectors, where both $\mathbf{U}$ and $\mathbf{V}$ are orthonormal matrices. Upon substituting (2.12) into (2.11), it is easy to see that the EOFs are given by $\boldsymbol{\Psi} = \mathbf{V}$, and $\boldsymbol{\Lambda} = \mathbf{D}'\mathbf{D}$. In addition, it is straightforward to show that $\mathbf{A} = (\sqrt{T-1})\mathbf{U}\mathbf{D}$ and that the first m columns of $(\sqrt{T-1})\mathbf{U}$ correspond to the normalized PC time series, $\mathbf{A}_{\mathrm{norm}}$. Thus, the advantages of the SVD calculation approach are: (1) we do not need to calculate the empirical spatial covariance matrix; (2) we get the normalized PC time series and EOFs simultaneously; and (3) the procedure still works when $T < m$. The case of $T < m$ can be problematic in the covariance context since then $\mathbf{C}_z^{(0)}$ is not positive-definite, although, as shown in Cressie and Wikle (2011, Section 5.3.4), in this case one can still calculate the EOFs and PC time series.

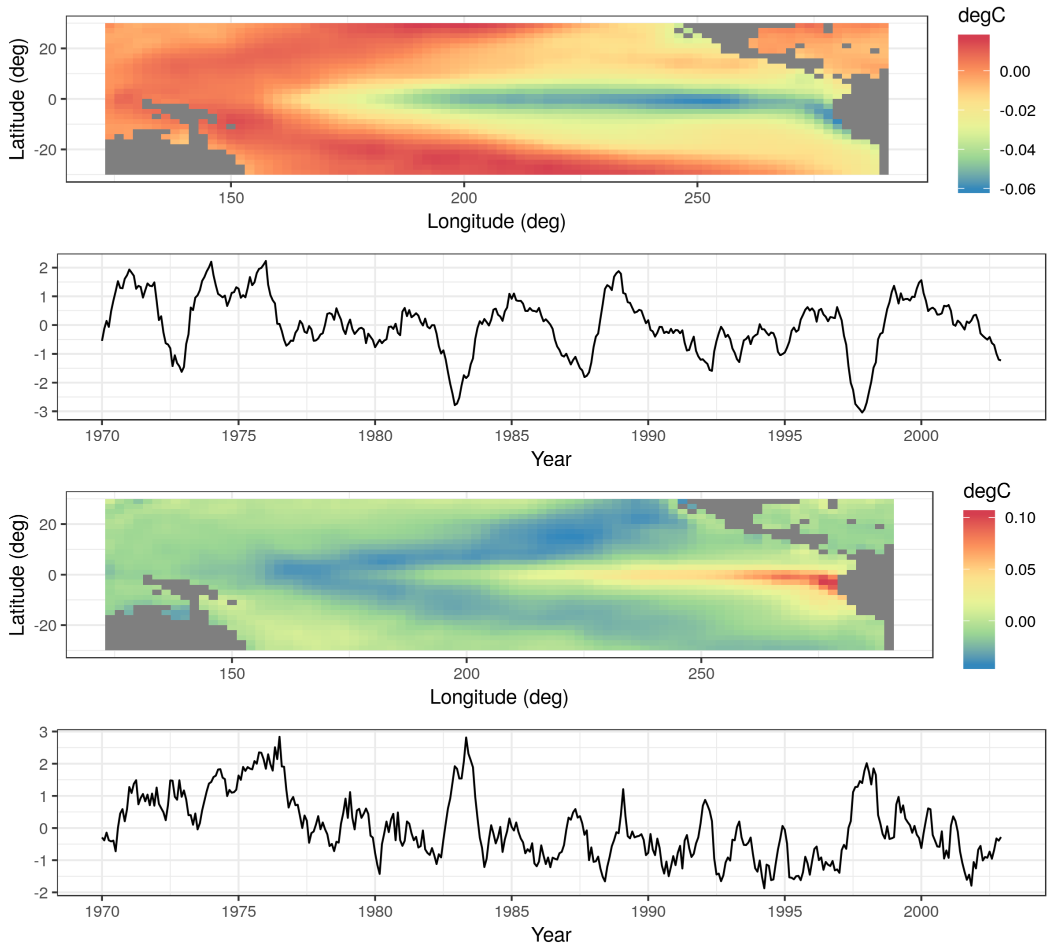

Figure 2.20: The first two empirical orthogonal functions and normalized principal-component time series for the SST data set obtained using an SVD of a space-wide matrix.

Figures 2.20 and 2.21 show the first four EOFs and PC time series for the SST data set. In this case, the number of spatial locations $m = 2261$, and the number of time points $T = 399$. The first four EOFs account for slightly more than 60% of the variation in the data. The EOF spatial patterns show strong variability in the eastern and central tropical Pacific, and they are known to be related to the El Niño and La Niña climate patterns that dominate the tropical Pacific SST variability. The corresponding PC time series (particularly for the first EOF) show time periods at which the data project very strongly on this spatial pattern (both in terms of large positive and large negative values), and it can be shown that these times correspond to strong El Niño and La Niña events, respectively.

How many EOFs should one consider? This is a long-standing question in PCA, and

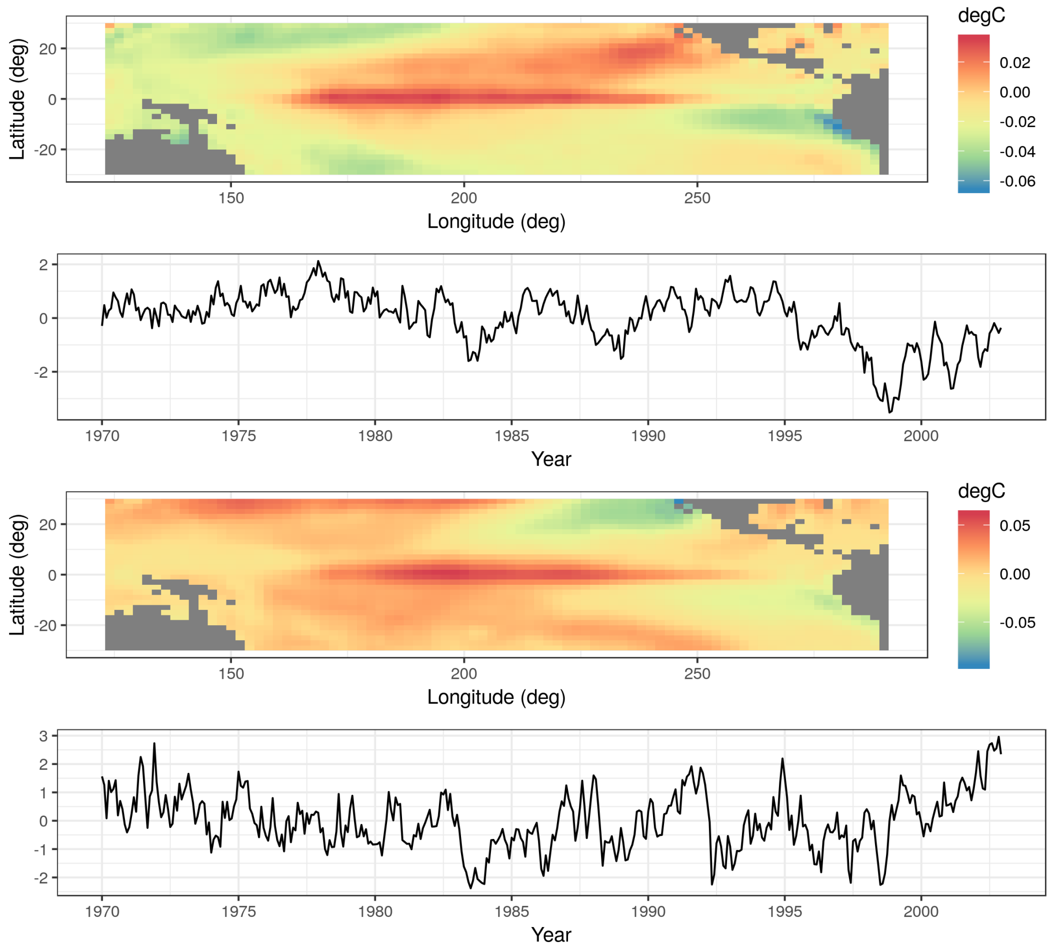

Figure 2.21: The third and fourth empirical orthogonal functions and normalized principal-component time series for the SST data set obtained using an SVD of a space-wide matrix.

there are numerous suggestions. Perhaps the simplest is just to consider the number of EOFs that account for some desired proportion of overall variance. Alternatively, one can produce a *scree plot*, which is a plot of the relative variance associated with each eigenvalue of the EOF as a function of the index of that EOF (see Figure 2.22), and where the sum of all relative variances is 1. One typically sees a fairly quick drop in relative variance with increasing order of the eigenvalue, and then the variance reduction flattens out. It is sometimes recommended that one only focus on those EOFs before the index that begins the flat part of the curve; this choice of index can be a bit subjective. One can also get a sense as to the "significance" of each component by comparing the relative variances to those in an EOF analysis in which the values for each spatial location are randomly permuted at each

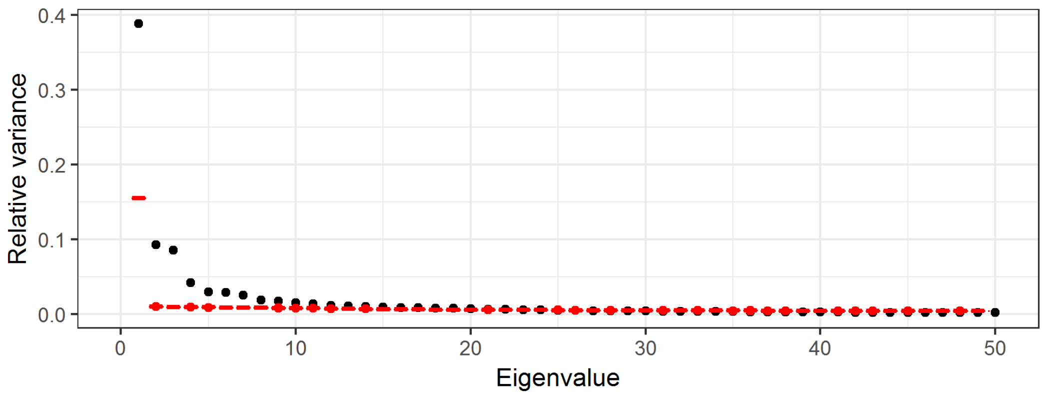

Figure 2.22: Scree plot for the EOF analysis of the SST data. The black symbols correspond to the relative variance associated with the ordered eigenvalues. The red symbols correspond to (very tight) boxplots of the relative variance associated with the eigenvalues from 100 EOF analyses in which the SST values at the spatial locations were randomly permuted for each time point.

time (see, for example, Hastie et al., 2009, Chapter 14). Then, one plots the scree plot with the actual data superimposed on the permuted data. We recommend that the EOFs retained are around the index at which the two "curves" intersect. For example, the black symbols in Figure 2.22 correspond to the relative variance associated with the first 50 EOFs for the SST data, and the red symbols are the very tight boxplots of relative variances obtained from EOF analyses of 100 random permutations of the data. One can see that by about index 12, the scree plot of the actual data and the boxplots are starting to intersect, suggesting that there is very little "real" variability being accounted for by the EOFs with indices greater than about 12.

Some Technical Comments on Empirical Orthogonal Functions

The EOF decomposition is sometimes derived in a continuous-space context through a Karhunen–Loève expansion, with eigenvalues and eigenfunctions obtained through a solution of a Fredholm integral equation (see the overview in Cressie and Wikle, 2011, Section 5.3). This is relevant, as it shows why one should account for the area/support associated with each spatial observation when working in a discrete-space EOF environment. In particular, one should multiply the elements of the eigenvectors by the square root of the length, area, or volume of the spatial support associated with that spatial observation (e.g., Cohen and Jones, 1969). For example, consider spatial location $\mathbf{s}_i$; for each of the k eigenvectors, one should multiply $\psi_k(\mathbf{s}_i)$ by $\sqrt{e_i}$, where e_i is the length, area, or volume associated with location $\mathbf{s}_i$ (and we assume that not all of the $\{e_i\}$ are identical). This modification to the eigenvectors $\boldsymbol{\psi}_1, \ldots, \boldsymbol{\psi}_k$ must be done before calculating the PC time series.

Although most EOF analyses in the spatio-temporal context consider spatial EOFs and PC time series, one can certainly consider the analogous decomposition in which the EOFs are time-series bases and the projection of the data onto these bases is given by PC spatial fields. Implementation is straightforward – one either works with the temporal covariance matrix (averaging over spatial location) or considers the SVD of an $m \times T$ (temporally detrended) data matrix. EOF time series are used as temporal basis functions in a spatio-temporal model in Lab 4.3.

It is also important to note that in cases where EOF analysis is used for dimension reduction (see Section 4.3), it is often necessary to either interpolate the EOFs in a sensible manner (e.g., Obled and Creutin, 1986) or "pre-interpolate" the data onto a finely gridded spatial domain.

Finally, there are many extensions to the basic EOF analysis presented here, including so-called complex EOFs, cyclostationary EOFs, multivariate EOFs, and extended EOFs. These all have particular utility depending on the type of data and the goal of the analysis. For example, complex EOFs are used for trying to identify propagating features that account for a significant amount of variation in the data. Cyclostationary EOFs are appropriate when there are strong periodicities in the data and spatial variation is expected to shift dramatically within this periodicity. Multivariate EOFs are considered when multivariate spatial data are observed at the same time points. Extended EOFs are useful for understanding spatial patterns associated with temporal lags. These methods are described in more detail in Cressie and Wikle (2011, Section 5.3) and the references therein. In Lab 2.3 we will demonstrate the "classic" EOF analysis in `R`.

2.4.4 Spatio-Temporal Canonical Correlation Analysis

In multivariate statistics, canonical correlation analysis (CCA) seeks to create new variables that are linear combinations of two multivariate data sets (separately) such that the correlations between these new variables are maximized (e.g., Hotelling, 1936). Such methods can be extended to the case where the two data sets are indexed in space and time, typically where a spatial location corresponds to a "trait" in a multivariate set of "traits" (this terminology is borrowed from psychometrics). Time corresponds to the samples. (Note that just as with EOFs, one can reverse the roles of space and time in this setting as well.) A spatio-temporal CCA (ST-CCA) is given below where spatial location corresponds to the multivariate trait.

Assume that we have two data sets that have the same temporal domain of interest but potentially different spatial domains. In particular, consider the data sets given by the collection of spatial vectors $\{\mathbf{Z}_{t_j} \equiv (Z(\mathbf{s}_1;t_j), \ldots, Z(\mathbf{s}_m;t_j))' : j = 1, \ldots, T\}$, and $\{\mathbf{X}_{t_j} \equiv (X(\mathbf{r}_1;t_j), \ldots, X(\mathbf{r}_n;t_j))' : j = 1, \ldots, T\}$. Now, consider the two new variables that are linear combinations of $\mathbf{Z}_{t_j}$ and $\mathbf{X}_{t_j}$, respectively:

$$a_k(t_j) = \sum_{i=1}^{m} \xi_{ik} \; Z(\mathbf{s}_i; t_j) = \boldsymbol{\xi}_k' \mathbf{Z}_{t_j}, \tag{2.13}$$

$$b_k(t_j) = \sum_{\ell=1}^{n} \psi_{\ell k} \; X(\mathbf{r}_\ell; t_j) = \boldsymbol{\psi}_k' \mathbf{X}_{t_j}. \tag{2.14}$$

For suitable choices of weights (see below), the kth *canonical correlation*, for $k = 1, 2, \ldots, \min\{n, m\}$, is then simply the correlation between a_k and b_k,

$$r_k \equiv \text{corr}(a_k, b_k) = \frac{\text{cov}(a_k, b_k)}{\sqrt{\text{var}(a_k)}\sqrt{\text{var}(b_k)}},$$

which can also be written as

$$r_k = \frac{\boldsymbol{\xi}_k' \mathbf{C}_{z,x}^{(0)} \boldsymbol{\psi}_k}{(\boldsymbol{\xi}_k' \mathbf{C}_z^{(0)} \boldsymbol{\xi}_k)^{1/2} (\boldsymbol{\psi}_k' \mathbf{C}_x^{(0)} \boldsymbol{\psi}_k)^{1/2}}, \tag{2.15}$$

where the variance–covariance matrices $\mathbf{C}_z^{(0)}$ and $\mathbf{C}_x^{(0)}$ are of dimension $m \times m$ and $n \times n$, respectively, and the cross-covariance matrix $\mathbf{C}_{z,x}^{(0)} \equiv \text{cov}(\mathbf{Z}, \mathbf{X})$ has dimension $m \times n$. So the first pair of canonical variables corresponds to the weights $\boldsymbol{\xi}_1$ and $\boldsymbol{\psi}_1$ that maximize r_1 in (2.15). In addition, we standardize these weights such that the new canonical variables have unit variance. Given this first pair of canonical variables, we can then find a second pair, $\boldsymbol{\xi}_2$ and $\boldsymbol{\psi}_2$, associated with $\{a_2, b_2\}$ that are uncorrelated with $\{a_1, b_1\}$, have unit variance, and maximize r_2 in (2.15). This procedure continues so that the kth set of canonical variables are the linear combinations, $\{a_k, b_k\}$, that have unit variance, are uncorrelated with the previous $k - 1$ canonical variable pairs, and maximize r_k in (2.15). A specific procedure for calculating ST-CCA is given in Technical Note 2.3.

Because the weights given by $\boldsymbol{\xi}_k$ and $\boldsymbol{\psi}_k$ are indexed in space, they can be plotted as spatial maps, and the associated canonical variables can be plotted as time series. From an interpretation perspective, the time series of the first few canonical variables typically match up fairly closely (given they are optimized to maximize correlation), and the spatial patterns in the weights show the areas in space that are most responsible for the high correlations. Like EOFs, principal components, and other such approaches, one has to be careful with the interpretation of canonical variables beyond the first pair, given the restriction that CCA time series are uncorrelated. In addition, given that high canonical correlations within a canonical pair naturally result from this procedure, one has to be careful in evaluating the importance of that correlation. One way to do this is to randomly permute the spatial locations in the $\mathbf{Z}_{t_j}$ and $\mathbf{X}_{t_j}$ data vectors (separately) and recalculate the ST-CCA many times, thereby giving a permutation-based range of canonical correlations when there is no real structural relationship between the variables.

In addition to the consideration of two separate data sets, one can perform an ST-CCA between $\mathbf{Z}_{t_j}$ and, say, $\mathbf{X}_{t_j} \equiv \mathbf{Z}_{t_j-\tau}$, a τ-lagged version of the $\mathbf{Z}_{t_j}$ data. This "one-field ST-CCA" is often useful for exploratory data analysis or for generating a forecast of a spatial field. Some binning of the spatio-temporal data into temporal bins lagged by τ may be needed in practice.

Finally, in practice, because the covariance matrices required to implement ST-CCA are often fairly noisy (and even singular), depending on the sample size, we typically first project the data into a lower dimension using EOFs for computational stability (see Cressie and Wikle, 2011, Section 5.6.1). This is the approach we take in Lab 2.3.

As an example of ST-CCA, we consider a one-field ST-CCA on the SST data set. In particular, we are interested in forecasting SST seven months in the future, so we let the data $\mathbf{X}$ be the lag $\tau = 7$ month SST data and the data $\mathbf{Z}$ be the same SSTs with no lag. However, because $T < \max\{m, n\}$ for these data, we first project the data onto the first 10 EOFs (which account for about 74% of the variance in the data). For the projected data, Figure 2.23 shows the first canonical variables (i.e., $\{a_1(t_j), b_1(t_j) : j = 1, \ldots, T\}$), plotted as individual time series and which correspond to a canonical correlation of $r_1 = 0.843$. Figure 2.24 shows the corresponding spatial-weights maps for $\boldsymbol{\xi}_1$ and $\boldsymbol{\psi}_1$, respectively. In this example, it can be seen from the time-series plots that the series are quite highly correlated, and it can be shown that the large peaks correspond to known El Niño Southern Oscillation (ENSO) events. Similarly, the left panel of Figure 2.24 suggests a precursor pattern to the SST field in the right panel.

Technical Note 2.3: Calculating ST-CCA

First, let $k = 1$ and, because $\mathbf{C}_z^{(0)}$ and $\mathbf{C}_x^{(0)}$ are positive-definite, note that we can write $\mathbf{C}_z^{(0)} = (\mathbf{C}_z^{(0)})^{1/2}(\mathbf{C}_z^{(0)})^{1/2}$ and $\mathbf{C}_x^{(0)} = (\mathbf{C}_x^{(0)})^{1/2}(\mathbf{C}_x^{(0)})^{1/2}$ (see Appendix A). Thus, from (2.15), the square of the canonical correlation can be written as

$$r_1^2 = \frac{[\widetilde{\boldsymbol{\xi}}_1'(\mathbf{C}_z^{(0)})^{-1/2}\mathbf{C}_{z,x}^{(0)}(\mathbf{C}_x^{(0)})^{-1/2}\widetilde{\boldsymbol{\psi}}_1]^2}{(\widetilde{\boldsymbol{\xi}}_1'\widetilde{\boldsymbol{\xi}}_1)(\widetilde{\boldsymbol{\psi}}_1'\widetilde{\boldsymbol{\psi}}_1)}, \tag{2.16}$$

with $\widetilde{\boldsymbol{\xi}}_1 \equiv (\mathbf{C}_z^{(0)})^{1/2}\boldsymbol{\xi}_1$ and $\widetilde{\boldsymbol{\psi}}_1 \equiv (\mathbf{C}_x^{(0)})^{1/2}\boldsymbol{\psi}_1$, the so-called normalized weights. The CCA problem is now solved if we can find the $\widetilde{\boldsymbol{\xi}}_1$ and $\widetilde{\boldsymbol{\psi}}_1$ that maximize (2.16). In the multivariate statistics literature (e.g., Johnson and Wichern, 1992, p. 463) it is well known that r_1^2 corresponds to the largest singular value of the singular value decomposition (SVD; see Appendix A) of

$$(\mathbf{C}_z^{(0)})^{-1/2}\mathbf{C}_{z,x}^{(0)}(\mathbf{C}_x^{(0)})^{-1/2}, \tag{2.17}$$

where the normalized weight vectors $\widetilde{\boldsymbol{\xi}}_1$ and $\widetilde{\boldsymbol{\psi}}_1$ are the left and right singular vectors, respectively. Then we can obtain the unnormalized weights, $\boldsymbol{\xi}_1$ and $\boldsymbol{\psi}_1$, through $\boldsymbol{\xi}_1 \equiv$

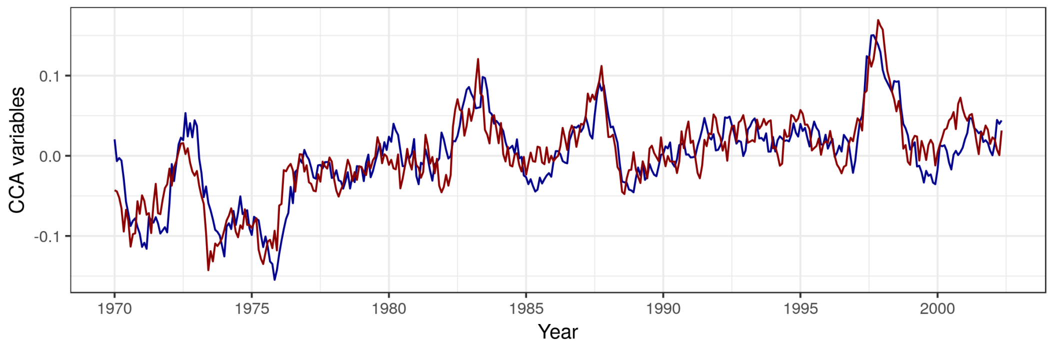

Figure 2.23: Time series of the first canonical variables, $\{a_1, b_1\}$, for $\tau = 7$ month lagged monthly SST anomalies at time $t_j - \tau$ (blue) and those at time t_j (red).

$(\mathbf{C}_z^{(0)})^{-1/2}\widetilde{\boldsymbol{\xi}}_1$ and $\boldsymbol{\psi}_1 \equiv (\mathbf{C}_x^{(0)})^{-1/2}\widetilde{\boldsymbol{\psi}}_1$, respectively. As mentioned above, these are the first ST-CCA pattern maps. The corresponding time series of ST-CCA canonical variables are then calculated directly from $a_1(t_j) = \boldsymbol{\xi}_1'\mathbf{Z}_{t_j}$ and $b_1(t_j) = \boldsymbol{\psi}_1'\mathbf{X}_{t_j}$, for $j = 1, \ldots, T$. More generally, $\widetilde{\boldsymbol{\xi}}_k$ and $\widetilde{\boldsymbol{\psi}}_k$ correspond to the left and right singular vectors associated with the kth singular value (r_k^2) in the SVD of (2.17). Then the unnormalized spatial-weights maps and the canonical time series are obtained analogously to the $k = 1$ case.

In practice, to evaluate the SVD in (2.17), we must first calculate the empirical covariance matrices $\widehat{\mathbf{C}}_z^{(0)}$, $\widehat{\mathbf{C}}_x^{(0)}$ using (2.4), as well as the empirical cross-covariance matrix $\widehat{\mathbf{C}}_{z,x}^{(0)}$ given by (2.5). Finally, we consider the SVD of $(\widehat{\mathbf{C}}_z^{(0)})^{-1/2}\widehat{\mathbf{C}}_{z,x}^{(0)}(\widehat{\mathbf{C}}_x^{(0)})^{-1/2}$. As mentioned in the text, the empirical covariance matrices can be unstable (or singular) unless $T \gg \max(n, m)$, and so it is customary to work in EOF space; that is, project the data for one or both variables onto a lower-dimensional space given by a relatively few EOFs before carrying out ST-CCA.

2.5 Chapter 2 Wrap-Up

There were three main goals in this chapter. First, we wanted to expose the reader to some basic ideas about data structures in R that are useful for working with spatio-temporal data. Next, we wanted to illustrate some useful ways to visualize spatio-temporal data, noting that it can be particularly challenging to visualize dynamical evolution of spatial fields either without collapsing the spatial component onto one spatial dimension (e.g., as with the Hovmöller plots) or through animation. Finally, we wanted to describe some standard

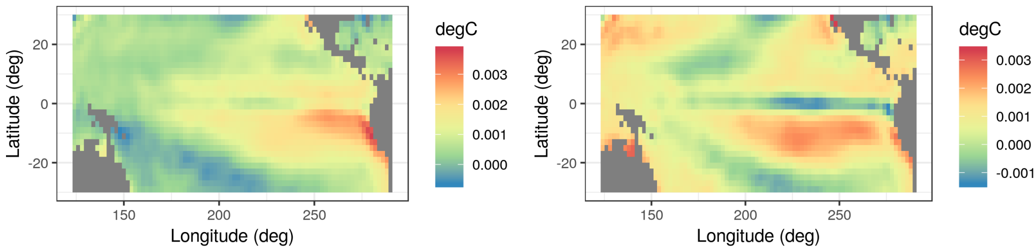

Figure 2.24: Spatial-weights maps corresponding to the linear combination of EOFs used to construct the canonical variables for SST data lagged $\tau = 7$ months (left) and the unlagged SST data (right).

ways to explore spatio-temporal data in preparation for developing models in Chapter 3. In particular, we discussed the exploration of the first moments (means) in space or time, and the second-order structures (covariances) either jointly in space and time, or averaged over one of the dimensions (usually the time dimension) to give covariance and cross-covariance matrices. Stepping up the technical level, we considered eigenvector approaches to explore the structure and potentially reduce the dimensionality of the spatio-temporal data. Specifically, we considered EOFs and ST-CCA. Of these, the EOFs are the most ubiquitous in the literature. Even if the technical details were a bit elaborate, the end result is a powerful and interpretable visualization and exploration of spatio-temporal variability.

You now have the survival skills to start building statistical models for spatio-temporal data, with the goal of spatial prediction, temporal forecasting, or parameter inference. In subsequent chapters, spatio-temporal statistical models will be discussed from an introductory perspective in Chapter 3, from a descriptive perspective in Chapter 4, and from a dynamic perspective in Chapter 5.

Lab 2.1: Data Wrangling

Spatio-temporal modeling and prediction generally involve substantial amounts of data that are available to the user in a variety of forms, but more often than not as tables in CSV files or text files. A considerable amount of time is usually spent in loading the data and pre-processing them in order to put them into a form that is suitable for analysis. Fortunately, there are several packages in `R` that help the user achieve these goals quickly; here we focus on the packages **dplyr** and **tidyr**, which contain functions particularly suited for the data manipulation techniques that are required. We first load the required packages, as well as **STRbook** (visit `https://spacetimewithr.org` for instructions on how to install **STRbook**).

```
library("dplyr")
library("tidyr")
library("STRbook")
```

As running example we will consider the NOAA data set, which was provided to us as text in tables and is available with the package **STRbook**. There are six data tables:

- `Stationinfo.dat`. This table contains 328 rows (one for each station) and three columns (station ID, latitude coordinate, and longitude coordinate) containing information on the stations' locations.
- `Times_1990.dat`. This table contains 1461 rows (one for each day between 01 January 1990 and 30 December 1993) and four columns (Julian date, year, month, day) containing the data time stamps.
- `Tmax_1990.dat`. This table contains 1461 rows (one for each time point) and 328 columns (one for each station location) containing all maximum temperature data with missing values coded as -9999.
- `Tmin_1990.dat`. Same as `Tmax_1990.dat` but containing minimum temperature data.
- `TDP_1990.dat`. Same as `Tmax_1990.dat` but containing temperature dew point data with missing values coded as -999.90001.
- `Precip_1990.dat`. Same as `Tmax_1990.dat` but containing precipitation data with missing values coded as -99.989998.

The first task is to reconcile all these data into one object. Before seeing how to use the spatio-temporal data classes to do this, we first consider the rather simpler task of reconciling them into a standard `R` data frame in long format.

Working with Spatio-Temporal Data in Long Format

The station locations, time stamps and maximum temperature data can be loaded into `R` from **STRbook** as follows.

```
locs <- read.table(system.file("extdata", "Stationinfo.dat",
                               package = "STRbook"),
                   col.names = c("id", "lat", "lon"))
Times <- read.table(system.file("extdata", "Times_1990.dat",
                                package = "STRbook"),
                    col.names = c("julian", "year", "month", "day"))
Tmax <- read.table(system.file("extdata", "Tmax_1990.dat",
                               package = "STRbook"))
```

In this case, **system.file** and its arguments are used to locate the data within the package **STRbook**, while **read.table** is the most important function used in R for reading data input from text files. By default, **read.table** assumes that data items are separated by a blank space, but this can be changed using the argument sep. Other important data input functions worth looking up include **read.csv** for comma-separated value files, and **read.delim**.

Above we have added the column names to the data locs and Times since these were not available with the original text tables. Since we did not assign column names to Tmax, the column names are the default ones assigned by **read.table**, that is, V1, V2, ..., V328. As these do not relate to the station ID in any way, we rename these columns as appropriate using the data in locs.

```
names(Tmax) <- locs$id
```

The other data can be loaded in a similar way to Tmax; we denote the resulting variables as Tmin, TDP, and Precip, respectively. One can, and should, use the functions **head** and **tail** to check that the loaded data are sensible.

Consider now the maximum-temperature data in the NOAA data set. Since each row in Tmax is associated with a time point, we can attach it columnwise to the data frame Times using **cbind**.

```
Tmax <- cbind(Times, Tmax)
head(names(Tmax), 10)

##  [1] "julian" "year"   "month"  "day"    "3804"   "3809"
##  [7] "3810"   "3811"   "3812"   "3813"
```

Now Tmax contains the time information in the first four columns and temperature data in the other columns. To put Tmax into long format we need to identify a *key–value* pair. In our case, the data are in space-wide format where the *keys* are the station IDs and the *values* are the maximum temperatures (which we store in a field named z). The function we use to put the data frame into long format is **gather**. This function takes the data as first argument, the key–value pair, and then the next arguments are the names of any columns to exclude as values (in this case those relating to the time stamp).

```
Tmax_long <- gather(Tmax, id, z, -julian, -year, -month, -day)
head(Tmax_long)

##   julian year month day   id  z
## 1 726834 1990     1   1 3804 35
## 2 726835 1990     1   2 3804 42
## 3 726836 1990     1   3 3804 49
## 4 726837 1990     1   4 3804 59
```

```
## 5 726838 1990      1    5 3804 41
## 6 726839 1990      1    6 3804 45
```

Note how **gather** has helped us achieve our goal: we now have a single row per measurement and multiple rows may be associated with the same time point. As is, the column `id` is of class `character` since it was extracted from the column names. Since the station ID is an integer it is more natural to ensure the field is of class `integer`.

```
Tmax_long$id <- as.integer(Tmax_long$id)
```

There is little use to keep missing data (coded as -9999 in our case) when the data are in long format. To filter out these data we can use the function **filter**. Frequently it is better to use an *inequality* criterion (e.g., less than) when filtering in this way rather than an *equivalence* criterion (is equal to) due to truncation error when storing data. This is what we do below, and filter out data with values less than -9998 rather than data with values equal to -9999. This is particularly important when processing the other variables, such as preciptation, where the missing value is -99.989998.

```
nrow(Tmax_long)

## [1] 479208

Tmax_long <- filter(Tmax_long, !(z <= -9998))
nrow(Tmax_long)

## [1] 196253
```

Note how the number of rows in our data set (returned from the function **nrow**) has now decreased by more than half. One may also use the `R` function **subset**; however, **filter** tends to be faster for large data sets. Both **subset** and **filter** take logical expression as instruction on how to filter out unwanted rows. As with **gather**, the column names in the logical expression do not appear as strings. In `R` this method of providing arguments is known as *non-standard evaluation*, and we shall see several instances of it in the course of the Labs.

Now assume we wish to include minimum temperature and the other variables inside this data frame too. The first thing we need to do is first make sure every measurement `z` is attributed to a process. In our case, we need to add a column, say `proc`, indicating what process the measurement relates to. There are a few ways in which to add a column to a data frame; here we shall introduce the function **mutate**, which will facilitate operations in the following Labs.

```
Tmax_long <- mutate(Tmax_long, proc = "Tmax")
head(Tmax_long)

##   julian year month day   id  z proc
## 1 726834 1990     1   1 3804 35 Tmax
## 2 726835 1990     1   2 3804 42 Tmax
## 3 726836 1990     1   3 3804 49 Tmax
## 4 726837 1990     1   4 3804 59 Tmax
## 5 726838 1990     1   5 3804 41 Tmax
## 6 726839 1990     1   6 3804 45 Tmax
```

Now repeat the same procedure with the other variables to obtain data frames `Tmin_long`, `TDP_long`, and `Precip_long` (remember the different codings for the missing values!). To save time, the resulting data frames can also be loaded directly from **STRbook** as follows.

```
data(Tmin_long, package = "STRbook")
data(TDP_long, package = "STRbook")
data(Precip_long, package = "STRbook")
```

We can now construct our final data frame in long format by simply concatenating all these (rowwise) together using the function **`rbind`**.

```
NOAA_df_1990 <- rbind(Tmax_long, Tmin_long, TDP_long, Precip_long)
```

There are many advantages of having data in long form. For example, it makes grouping and summarizing particularly easy. Let us say we want to find the mean value for each variable in each year. We do this using the functions **`group_by`** and **`summarise`**. The function **`group_by`** creates a *grouped data frame*, while **`summarise`** does an operation *on each group within the grouped data frame*.

```
summ <- group_by(NOAA_df_1990, year, proc) %>%  # groupings
        summarise(mean_proc = mean(z))          # operation
```

Alternatively, we may wish to find out the number of days on which it did not rain at each station in June of every year. We can first filter out the other variables and then use **`summarise`**.

```
NOAA_precip <- filter(NOAA_df_1990, proc == "Precip" & month == 6)
summ <- group_by(NOAA_precip, year, id) %>%
        summarise(days_no_precip = sum(z == 0))
head(summ)
```

```
## # A tibble: 6 x 3
## # Groups:   year [1]
##    year    id days_no_precip
##   <int> <int>          <int>
## 1  1990  3804             19
## 2  1990  3810             26
## 3  1990  3811             21
## 4  1990  3812             24
## 5  1990  3813             25
## 6  1990  3816             23
```

The median number of days with no recorded precipitation was

```
median(summ$days_no_precip)

## [1] 20
```

In the R code above, we have used the operator `%>%`, known as the *pipe* operator. This operator has its own nuances and should be used with care, but we find it provides a clear desciption of the processing pipeline a data set is passed through. We shall always use this operator as `x %>% f(y)`, which is shorthand for `f(x,y)`. For example, the June summaries above can be found equivalently using the commands

```
grps <- group_by(NOAA_precip, year, id)
summ <- summarise(grps, days_no_precip = sum(z == 0))
```

There are other useful commands in **dplyr** that we use in other Labs. First, the function `arrange` sorts by a column. For example, `NOAA_df_1990` is sorted first by station ID, and then by time (Julian date). The following code sorts the data first by time and then by station ID.

```
NOAA_df_sorted <- arrange(NOAA_df_1990, julian, id)
```

Calling `head(NOAA_df_sorted)` reveals that no measurements on temperature dew point are available for the first few days of the data set.

Another useful function is `select`, which can be used to select or discard columns. For example, in the following, `df1` selects only the Julian date and the measurement while `df2` contains all columns except the Julian date.

```
df1 <- select(NOAA_df_1990, julian, z)
df2 <- select(NOAA_df_1990, -julian)
```

At present, our long data frame contains no spatial information attached to it. However, for each station ID we have an associated coordinate in the data frame `locs`. We can merge locs to NOAA_df_1990 using the function **left_join**; this is considerably faster than the function **merge**. With **left_join** we need to supply the column field name by which we are merging. In our case, the field common to both data sets is "id".

```
NOAA_df_1990 <- left_join(NOAA_df_1990, locs, by = "id")
```

Finally, it may be the case that one wishes to revert from long format to either space-wide or time-wide format. The reverse function of **gather** is **spread**. This also works by identifying the key–value pair in the data frame; the values are then "widened" into a table while the keys are used to label the columns. For example, the code below constructs a space-wide data frame of maximum temperatures, with each row denoting a different date and each column containing data z from a specific station id.

```
Tmax_long_sel <- select(Tmax_long, julian, id, z)
Tmax_wide <- spread(Tmax_long_sel, id, z)
dim(Tmax_wide)

## [1] 1461  138
```

The first column is the Julian date. Should one wish to construct a standard matrix containing these data, then one can simply drop this column and convert as follows.

```
M <- select(Tmax_wide, -julian) %>% as.matrix()
```

Working with Spatio-Temporal Data Classes

Next, we convert the data into objects of class STIDF and STFDF; in these class names "DF" is short for "data frame," which indicates that in addition to the spatio-temporal locations (which only need STI or STF objects), the objects will also contain data. These classes are defined in the package **spacetime**. Since sometimes we construct spatio-temporal objects using spatial objects we also need to load the package **sp**. For details on these classes see Pebesma (2012).

```
library("sp")
library("spacetime")
```

Constructing an STIDF Object

The spatio-temporal object for irregular data, STIDF, can be constructed using two functions: **stConstruct** and **STIDF**. Let us focus on the maximum temperature in Tmax_long. The only thing we need to do before we call **stConstruct** is to define a formal time stamp from the year,month,day fields. First, we construct a field with the date in `year–month–day` format using the function **paste**, which concatenates strings together. Instead of typing `NOAA_df_1990$year, NOAA_df_1990$month` and `NOAA_df_1990$day` we embed the **paste** function within the function **with** to reduce code length.

```
NOAA_df_1990$date <- with(NOAA_df_1990,
                          paste(year, month, day, sep = "-"))
head(NOAA_df_1990$date, 4)    # show first four elements

## [1] "1990-1-1" "1990-1-2" "1990-1-3" "1990-1-4"
```

The field `date` is of type `character`. This field can now be converted into a `Date` object using **as.Date**.

```
NOAA_df_1990$date <- as.Date(NOAA_df_1990$date)
class(NOAA_df_1990$date)

## [1] "Date"
```

Now we have everything in place to construct the spatio-temporal object of class `STIDF` for maximum temperature. The easiest way to do this is using **stConstruct**, in which we provide the data frame in long format and indicate which are the spatial and temporal coordinates. This is the bare minimum required for constructing a spatio-temporal data set.

```
Tmax_long2 <- filter(NOAA_df_1990, proc == "Tmax")
STObj <- stConstruct(x = Tmax_long2,            # data set
                     space = c("lon", "lat"),  # spatial fields
                     time = "date")            # time field
class(STObj)

## [1] "STIDF"
## attr(,"package")
## [1] "spacetime"
```

The function **class** can be used to confirm we have successfully generated an object of class `STIDF`. There are several other options that can be used with **stConstruct**. For example, one can set the coordinate reference system or specify whether the time field indicates an instance or an interval. Type **help**`(stConstruct)` into the `R` console for more details.

The function **STIDF** is slightly different from **stConstruct** as it requires one to also specify the spatial part as an object of class `Spatial` from the package **sp**. In our case, the spatial component is simply an object containing irregularly spaced data, which in the package **sp** is a `SpatialPoints` object. A `SpatialPoints` object may be constructed using the function **SpatialPoints** and by supplying the coordinates as arguments. As with **stConstruct**, several other arguments can also be supplied to **SpatialPoints**; see the help file of **SpatialPoints** for more details.

```
spat_part <- SpatialPoints(coords = Tmax_long2[, c("lon", "lat")])
temp_part <- Tmax_long2$date
STObj2 <- STIDF(sp = spat_part,
                time = temp_part,
                data = select(Tmax_long2, -date, -lon, -lat))
class(STObj2)

## [1] "STIDF"
## attr(,"package")
## [1] "spacetime"
```

Constructing an STFDF Object

A similar approach can be used to construct an `STFDF` object instead of an `STIDF` object. When the spatial points are fixed in time, we only need to provide as many spatial coordinates as there are spatial points, in this case those of the station locations. We also need to provide the regular time stamps, that is, one for each day between 01 January 1990 and 30 December 1993. Finally, the data can be provided both in space-wide or time-wide format with **stConstruct**, and in long format with **STFDF**. Here we show how to use **STFDF**.

The spatial and temporal parts can be obtained from the original data as follows.

```
spat_part <- SpatialPoints(coords = locs[, c("lon", "lat")])
temp_part <- with(Times,
                  paste(year, month, day, sep = "-"))
temp_part <- as.Date(temp_part)
```

The data need to be provided in long format, but now they must contain all the missing values too since a data point must be provided for every spatial and temporal combination. To get the data into long format we use **gather**.

```
Tmax_long3 <- gather(Tmax, id, z, -julian, -year, -month, -day)
```

It is very important that the data frame in long format supplied to **STFDF** has the spatial index moving faster than the temporal index, and that the order of the spatial index is the same as that of the spatial component supplied.

```
Tmax_long3$id <- as.integer(Tmax_long3$id)
Tmax_long3 <- arrange(Tmax_long3,julian,id)
```

Confirming that the spatial ordering in `Tmax_long3` is the correct one can be done as follows.

```
all(unique(Tmax_long3$id) == locs$id)

## [1] TRUE
```

We are now ready to construct the `STFDF`.

```
STObj3 <- STFDF(sp = spat_part,
                time = temp_part,
                data = Tmax_long3)
class(STObj3)

## [1] "STFDF"
## attr(,"package")
## [1] "spacetime"
```

Since we will be using `STObj3` often in the Labs we further equip it with a coordinate reference system (see Bivand et al., 2013, for details on these reference systems),

```
proj4string(STObj3) <- CRS("+proj=longlat +ellps=WGS84")
```

and replace the missing values (currently coded as -9999) with `NA`s.

```
STObj3$z[STObj3$z == -9999] <- NA
```

For ease of access, this object is saved as a data file in **STRbook** and can be loaded using the command `data("STObj3", package = "STRbook")`.

Lab 2.2: Visualization

In this Lab we shall visualize maximum temperature data in the NOAA data set. Specifically, we consider the maximum recorded temperature between May 1993 and September 1993 (inclusive). The packages we need are **animation**, **dplyr**, **ggplot2**, **gstat**, **maps**, and **STRbook**.

```
library("animation")
library("dplyr")
library("ggplot2")
library("gstat")
library("maps")
library("STRbook")
```

In order to ensure consistency of results and visualizations we fix the seed to 1.

```
set.seed(1)
```

We now load the data set and take a subset of it using the function `filter`.

```
data("NOAA_df_1990", package = "STRbook")
Tmax <- filter(NOAA_df_1990,       # subset the data
               proc == "Tmax" &    # only max temperature
               month %in% 5:9 &    # May to September
               year == 1993)       # year of 1993
```

The data frame we shall work with is hence denoted by `Tmax`. The first six records in `Tmax` are:

```
Tmax %>% select(lon, lat, date, julian, z) %>% head()

##          lon   lat       date julian  z
## 1 -81.43333 39.35 1993-05-01 728050 82
## 2 -81.43333 39.35 1993-05-02 728051 84
## 3 -81.43333 39.35 1993-05-03 728052 79
## 4 -81.43333 39.35 1993-05-04 728053 72
## 5 -81.43333 39.35 1993-05-05 728054 73
## 6 -81.43333 39.35 1993-05-06 728055 78
```

The first record has a Julian date of 728050, corresponding to 01 May 1993. To ease the following operations, we create a new variable `t` that is equal to 1 when `julian == 728050` and increases by 1 for each day in the record.

```
Tmax$t <- Tmax$julian - 728049     # create a new time variable
```

The first task faced by the spatio-temporal modeler is data visualization. This is an important preliminary task that needs to be carried out prior to the exploratory-data-analysis stage and the modeling stages. Throughout, we shall make extensive use of the *grammar of graphics* package **ggplot2**, which is a convenient way to plot and visualize data and results in `R`. The book by Wickham (2016) provides a comprehensive introduction to **ggplot2**.

Spatial Plots

Visualization techniques vary with the data being analyzed. The NOAA data are collected at stations that are fixed in space; therefore, initial plots should give the modeler an idea of the overall spatial variation of the observed data. If there are many time points, usually only a selection of time points are chosen for visualization. In this case we choose three time points.

```
Tmax_1 <- subset(Tmax, t %in% c(1, 15, 30))  # extract data
```

The variable `Tmax_1` contains the data associated with the first, fifteenth, and thirtieth day in `Tmax`. We now plot this data subset using **ggplot2**. Note that the function `col_scale`, below, is simply a wrapper for the **ggplot2** function `scale_colour_distiller`, and is provided with **STRbook**.

```
NOAA_plot <- ggplot(Tmax_1) +                # plot points
    geom_point(aes(x = lon,y = lat,          # lon and lat
                   colour = z),              # attribute color
               size = 2) +                   # make all points larger
    col_scale(name = "degF") +               # attach color scale
    xlab("Longitude (deg)") +                # x-axis label
    ylab("Latitude (deg)") +                 # y-axis label
    geom_path(data = map_data("state"),      # add US states map
          aes(x = long, y = lat, group = group)) +
    facet_grid(~date) +                      # facet by time
    coord_fixed(xlim = c(-105, -75),
                ylim = c(25, 50))  +         # zoom in
    theme_bw()                               # B&W theme
```

`NOAA_plot` is a plot of the spatial locations of the stations. The function `aes` (short for aesthetics) for `geom_point` identifies which field in the data frame `Tmax_1` is the x-coordinate and which is the y-coordinate. **ggplot2** also allows one to attribute color (and size, if desired) to other fields in a similar fashion. The command `print(NOAA_plot)` generates the figure shown in Figure 2.1. As can be seen, the stations are approximately regularly spaced within the domain.

When working with geographic data, it is also good practice to put the spatial locations of the data into perspective, by plotting country or state boundaries together with the data locations. Above, the US state boundaries are obtained from the **maps** package through the command `map_data("state")`. The boundaries are then overlayed on the plot using `geom_path`, which simply joins the points and draws the resulting path with `x` against `y`. Projections can be applied by adding another layer to the **ggplot2** object using `coord_map`. For example adding + `coord_map(projection = "sinusoidal")` will plot using a sinusoidal projection. One can also plot in three dimensions by using `projection = "ortho"`.

In this example we have used **ggplot2** to plot *point-referenced data*. Plots of regular lattice data, such as those shown in Figure 2.2, are generated similarly by using `geom_tile` instead. Plots of irregular lattice data are generated using `geom_polygon`. As an example of the latter, consider the BEA income data set. These data can be loaded from **STRbook** as follows.

```
data("BEA", package = "STRbook")
head(BEA %>% select(-Description), 3)

##          NAME10 X1970 X1980 X1990
## 6      Adair, MO  2723  7399 12755
## 9     Andrew, MO  3577  7937 15059
## 12 Atchison, MO  3770  5743 14748
```

From the first three records, we can see that the data set contains the personal income, in dollars, by county and by year for the years 1970, 1980 and 1990. These data need to be merged with Missouri county data which contain geospatial information. These county data, which are also available in **STRbook**, were originally processed from a shapefile that was freely available online.[6]

```
data("MOcounties", package = "STRbook")
head(MOcounties %>% select(long, lat, NAME10), 3)

##       long     lat    NAME10
## 1 627911.9 4473554 Clark, MO
## 2 627921.4 4473559 Clark, MO
## 3 627923.0 4473560 Clark, MO
```

The data set contains the boundary points for the counties, amongst several other variables which we do not explore here. For example, to plot the boundary of the first county one can simply type

```
County1 <- filter(MOcounties, NAME10 == "Clark, MO")
plot(County1$long, County1$lat)
```

To add the BEA income data to the county data containing geospatial information we use `left_join`.

```
MOcounties <- left_join(MOcounties, BEA, by = "NAME10")
```

Now it is just a matter of calling `ggplot` with `geom_polygon` to display the BEA income data as spatial polygons. We also use `geom_path` to draw the county boundaries. Below we show the code for 1970; similar code would be needed for 1980 and 1990. Note the use of the `group` argument to identify which points correspond to which county. The resulting plots are shown in Figure 2.4.

[6] http://msdis-archive.missouri.edu/archive/metadata_gos/MO_2010_TIGER_Census_County_Boundaries.xml

```
g1 <- ggplot(MOcounties) +
    geom_polygon(aes(x = long, y = lat,         # county boundary
                     group = NAME10,            # county group
                     fill = log(X1970))) +      # log of income
    geom_path(aes(x = long, y = lat,            # county boundary
                  group = NAME10)) +            # county group
    fill_scale(limits = c(7.5,10.2),
               name = "log($)")  +
    coord_fixed() + ggtitle("1970") +           # annotations
    xlab("x (m)") + ylab("y (m)") + theme_bw()
```

Type `print(g1)` in the R console to display the plot.

Time-Series Plots

Next, we look at the time series associated with the maximum temperature data in the NOAA data set. One can plot the time series at all 139 weather stations (and this is recommended); here we look at the time series at a set of stations selected at random. We first obtain the set of unique station identifiers, choose 10 at random from these, and extract the data associated with these 10 stations from the data set.

```
UIDs <- unique(Tmax$id)                         # extract IDs
UIDs_sub <- sample(UIDs, 10)                    # sample 10 IDs
Tmax_sub <- filter(Tmax, id %in% UIDs_sub)      # subset data
```

To visualize the time series at these stations, we use *facets*. When given a long data frame, one can first subdivide the data frame into groups and generate a plot for each group. The following code displays the time series at each station. The command we use is `facet_wrap`, which automatically adjusts the number of rows and columns in which to display the facets. The command `facet_grid` instead uses columns for one grouping variable and rows for a second grouping variable, if specified.

```
TmaxTS <- ggplot(Tmax_sub) +
    geom_line(aes(x = t, y = z)) + # line plot of z against t
    facet_wrap(~id, ncol = 5) +    # facet by station
    xlab("Day number (days)") +    # x label
    ylab("Tmax (degF)") +          # y label
    theme_bw() +                   # BW theme
    theme(panel.spacing = unit(1, "lines")) # facet spacing
```

The argument `~id` supplied to `facet_wrap` is a `formula` in R. In this case, the formula is used to denote the groups by which we are faceting. The syntax `x~y` can be used to facet by two variables. The command `print(TmaxTS)` produces Figure 2.9.

Hovmöller Plots

A Hovmöller plot is a two-dimensional space-time visualization, where space is collapsed (projected or averaged) onto one dimension; the second dimension then denotes time. A Hovmöller plot can be generated relatively easily if the data are on a space-time grid, but unfortunately this is rarely the case! This is where data-wrangling techniques such as those explored in Lab 2.1 come in handy.

Consider the latitudinal Hovmöller plot. The first step is to generate a regular grid of, say, 25 spatial points and 100 temporal points using the function **expand.grid**, with limits set to the latitudinal and temporal limits available in the data set.

```
lim_lat <- range(Tmax$lat)          # latitude range
lim_t <- range(Tmax$t)              # time range
lat_axis <- seq(lim_lat[1],         # latitude axis
                lim_lat[2],
                length=25)
t_axis <- seq(lim_t[1],             # time axis
              lim_t[2],
              length=100)
lat_t_grid <- expand.grid(lat = lat_axis,
                          t = t_axis)
```

We next need to associate each station's latitudinal coordinate with the closest one on the grid. This can be done by finding the distance from the station's latitudinal coordinate to each point of the grid, finding which gridpoint is the closest, and allocating that to it. We store the gridded data in `Tmax_grid`.

```
Tmax_grid <- Tmax
dists <- abs(outer(Tmax$lat, lat_axis, "-"))
Tmax_grid$lat <- lat_axis[apply(dists, 1, which.min)]
```

Now that we have associated each station with a latitudinal coordinate, all that is left is to group by latitude and time, and then we average all station values falling in the latitude–time bands.

```
Tmax_lat_Hov <- group_by(Tmax_grid, lat, t) %>%
                summarise(z = mean(z))
```

In this case, every latitude–time band contains at least one data point, so that the Hovmöller plot contains no missing points on the established grid. This may not always be the case, and simple interpolation methods, such as **interp** from the **akima** package, can be used to fill out grid cells with no data.

Plotting gridded data is facilitated using the **ggplot2** function **geom_tile**. The function **geom_tile** is similar to **geom_point**, except that it assumes regularly spaced data and automatically uses rectangular patches in the plot. Since rectangular patches are "filled," we use the **STRbook** function **fill_scale** instead of **col_scale**, which takes the legend title in the argument `name`.

```
Hovmoller_lat <- ggplot(Tmax_lat_Hov) +            # take data
        geom_tile(aes(x = lat, y = t, fill = z)) + # plot
        fill_scale(name = "degF") +      # add color scale
        scale_y_reverse() +              # rev y scale
        ylab("Day number (days)") +      # add y label
        xlab("Latitude (degrees)") +     # add x label
        theme_bw()                       # change theme
```

The function **scale_y_reverse** ensures that time increases from top to bottom, as is typical in Hovmöller plots. We can generate a longitude-based Hovmöller plot in the same way. The resulting Hovmöller plots are shown in Figure 2.11.

Animations

To generate an animation in `R`, one can use the package **animation**. First, we define a function that plots a spatial map of the maximum temperature as a function of time:

```
Tmax_t <- function(tau) {
    Tmax_sub <- filter(Tmax, t == tau)        # subset data
    ggplot(Tmax_sub) +
        geom_point(aes(x = lon,y = lat, colour = z),   # plot
                   size = 4) +                         # pt. size
        col_scale(name = "z", limits = c(40, 110)) +
        theme_bw() # B&W theme
}
```

The function above takes a day number `tau`, filters the data frame according to the day number, and then plots the maximum temperature at the stations as a spatial map.

Next, we construct a function that plots the data for every day in the data set. The function that generates the animation within an HTML webpage is **saveHTML**. This takes the function that plots the sequence of images and embeds them in a webpage (by default named `index.html`) using JavaScript. The function **saveHTML** takes many arguments; type the command

```
help(saveHTML)
```

in the `R` console for more details.

```
gen_anim <- function() {
    for(t in lim_t[1]:lim_t[2]){   # for each time point
       plot(Tmax_t(t))             # plot data at this time point
    }
}

ani.options(interval = 0.2)      # 0.2s interval between frames
saveHTML(gen_anim(),             # run the main function
         autoplay = FALSE,       # do not play on load
         loop = FALSE,           # do not loop
         verbose = FALSE,        # no verbose
         outdir = ".",           # save to current dir
         single.opts = "'controls': ['first', 'previous',
                                     'play', 'next', 'last',
                                      'loop', 'speed'],
                                      'delayMin': 0",
         htmlfile = "NOAA_anim.html")  # save filename
```

To view the animation, load `NOAA_anim.html` from your working directory. The animation reveals dynamics within the spatio-temporal data that are not apparent using other visualization methods. For example, the maximum temperature clearly drifts from west to east at several points during the animation. This suggests that a dynamic spatio-temporal model that can capture this drift could provide a good fit to these data.

Lab 2.3: Exploratory Data Analysis

In this Lab we carry out exploratory data analysis (EDA), which typically requires visualization techniques similar to those utilized in Lab 2.2. There are several ways in which to carry out EDA with spatio-temporal data; in this Lab we consider the construction and visualization of the empirical means and covariances, the use of empirical orthogonal functions and their associated principal component time series, semivariogram analysis, and spatio-temporal canonical correlation analysis.

For the first part of the Lab, as in Lab 2.2, we shall consider the daily maximum temperatures in the NOAA data set between May 1993 and September 1993 (inclusive). The packages we need are **CCA, dplyr, ggplot2, gstat, sp, spacetime, STRbook** and **tidyr**.

```
library("CCA")
library("dplyr")
library("ggplot2")
library("gstat")
library("sp")
library("spacetime")
library("STRbook")
```

```
library("tidyr")
```

In order to ensure consistency of results and visualizations, we fix the seed to 1.

```
set.seed(1)
```

We now load the NOAA data set using the **data** command. To keep the data size manageable, we take a subset of it corresponding to the maximum daily temperatures in the months May–September 1993. As in Lab 2.2 we also add a new variable `t` which starts at 1 at the beginning of the data set and increases by 1 each day.

```
data("NOAA_df_1990", package = "STRbook")
Tmax <- filter(NOAA_df_1990,       # subset the data
               proc == "Tmax" &    # only max temperature
               month %in% 5:9 &    # May to September
               year == 1993)       # year of 1993
Tmax$t <- Tmax$julian - 728049     # create a new time variable
```

Empirical Spatial Means

The empirical spatial mean of our data is given by (2.1). The empirical spatial mean is a spatial quantity that can be stored in a new data frame that contains the spatial locations and the respective average maximum temperature at each location. These, and other data manipulations to follow, can be carried out easily using the tools we learned in Lab 2.1. We group by longitude and latitude, and then we compute the average maximum temperature at each of the separate longitude–latitude coordinates.

```
spat_av <- group_by(Tmax, lat, lon) %>%      # group by lon-lat
           summarise(mu_emp = mean(z))       # mean for each lon-lat
```

We can now plot the average maximum temperature per station and see how this varies according to longitude and latitude. The following plots are shown in Figure 2.14.

```
lat_means <- ggplot(spat_av) +
             geom_point(aes(lat, mu_emp)) +
             xlab("Latitude (deg)") +
             ylab("Maximum temperature (degF)") + theme_bw()

lon_means <- ggplot(spat_av) +
             geom_point(aes(lon, mu_emp)) +
             xlab("Longitude (deg)") +
             ylab("Maximum temperature (degF)") + theme_bw()
```

Empirical Temporal Means

We now generate the plot of Figure 2.15. The empirical temporal mean can be computed easily using the tools we learned in Lab 2.1: first, group the data by time; and second, summarize using the **summarise** function.

```
Tmax_av <- group_by(Tmax, date) %>%
           summarise(meanTmax = mean(z))
```

The variable `Tmax_av` is a data frame containing the average maximum temperature on each day (averaged across all the stations). This can be visualized easily, together with the original raw data, using **ggplot2**.

```
gTmaxav <-
    ggplot() +
    geom_line(data = Tmax,aes(x = date, y = z, group = id),
              colour = "blue", alpha = 0.04) +
    geom_line(data = Tmax_av, aes(x = date, y = meanTmax)) +
    xlab("Month") + ylab("Maximum temperature (degF)") +
    theme_bw()
```

Empirical Covariances

Before obtaining the empirical covariances, it is important that all trends are removed (not just the intercept). One simple way to do this is to first fit a linear model (that has spatial and/or temporal covariates) to the data. Then plot the empirical covariances of the detrended data (i.e., the residuals). Linear-model fitting proceeds with use of the **lm** function in `R`. The residuals from **lm** can then be incorporated into the original data frame `Tmax`.

In the plots of Figure 2.9 we observed a quadratic tendency of temperature over the chosen time span. Therefore, in what follows, we consider time and time squared as covariates. Note the use of the function **I**. This is required for `R` to interpret the power sign "^" as an arithmetic operator instead of a formula operator.

```
lm1 <- lm(z ~ lat + t + I(t^2), data = Tmax) # fit a linear model
Tmax$residuals <- residuals(lm1)              # store the residuals
```

We also need to consider the spatial locations of the stations, which we extract from `Tmax` used above.

```
spat_df <- filter(Tmax, t == 1) %>% # lon/lat coords of stations
             select(lon, lat)  %>%  # select lon/lat only
             arrange(lon, lat)      # sort ascending by lon/lat
m <- nrow(spat_av)                  # number of stations
```

The most straightforward way to compute the empirical covariance matrix (2.4) is using the `cov` function in `R`. When there are missing data, the usual way forward is to drop all records that are not complete (provided there are not too many of these). Specifically, if any of the elements in $\mathbf{Z}_{t_j}$ or $\mathbf{Z}_{t_j-\tau}$ are missing, the associated term in the summation of (2.4) is ignored altogether. The function `cov` implements this when the argument `use = 'complete.obs'` is supplied. If there are too many records that are incomplete, imputation, or the consideration of only subsets of stations, might be required.

In order to compute the empirical covariance matrices, we first need to put the data into space-wide format using `spread`.

```
X <- select(Tmax, lon, lat, residuals, t) %>% # select columns
     spread(t, residuals) %>%                 # make time-wide
     select(-lon, -lat) %>%                   # drop coord info
     t()                                      # make space-wide
```

Now it is simply a matter of calling `cov(X, use = 'complete.obs')` for computing the lag-0 empirical covariance matrix. For the lag-1 empirical covariance matrix we compute the covariance between the residuals from `X` excluding the first time point and `X` excluding the last time point.

```
Lag0_cov <- cov(X, use = 'complete.obs')
Lag1_cov <- cov(X[-1, ], X[-nrow(X),], use = 'complete.obs')
```

In practice, it is very hard to gain any intuition from these matrices, since points in a two-dimensional space do not have any specific ordering. One can, for example, order the stations by longitude and then plot the permuted spatial covariance matrix, but this works best when the domain of interest is rectangular with a longitude span that is much larger than the latitude span. In our case, with a roughly square domain, a workaround is to split the domain into either latitudinal or longitudinal strips, and then plot the spatial covariance matrix associated with each strip. In the following, we split the domain into four longitudinal strips (similar code can be used to generate latitudinal strips).

```
spat_df$n <- 1:nrow(spat_df)      # assign an index to each station
lim_lon <- range(spat_df$lon)     # range of lon coordinates
lon_strips <- seq(lim_lon[1],     # create 4 long. strip boundaries
                  lim_lon[2],
                  length = 5)
spat_df$lon_strip <- cut(spat_df$lon,       # bin the lon into
                         lon_strips,        # their respective bins
                         labels = FALSE,    # don't assign labels
                         include.lowest = TRUE) # include edges
```

The first six records of `spat_df` are:

```
head(spat_df)    # print the first 6 records of spat_df

##          lon      lat n lon_strip
## 1 -99.96667 37.76667 1         1
## 2 -99.76667 36.30000 2         1
## 3 -99.68333 32.43333 3         1
## 4 -99.05000 35.00000 4         1
## 5 -98.81667 38.86666 5         1
## 6 -98.51667 33.98333 6         1
```

Now that we know in which strip each station falls, we can subset the station data frame by strip and then sort the subsetted data frame by latitude. In **STRbook** we provide a function `plot_cov_strips` that takes an empirical covariance matrix `C` and a data frame in the same format as `spat_df`, and then plots the covariance matrix associated with each longitudinal strip. Plotting requires the package **fields**. We can plot the resulting lag-0 and lag-1 covariance matrices using the following code.

```
plot_cov_strips(Lag0_cov, spat_df)  # plot the lag-0 matrices
plot_cov_strips(Lag1_cov, spat_df)  # plot the lag-1 matrices
```

As expected (see Figure 2.16), the empirical spatial covariance matrices reveal the presence of spatial correlation in the residuals. The four lag-0 plots seem to be qualitatively similar, suggesting that there is no strong dependence on longitude. However, there is a dependence on latitude, and the spatial covariance appears to decrease with decreasing latitude. This dependence is a type of spatial *non-stationarity*, and such plots can be used to assess whether non-stationary spatio-temporal models are required or not.

Similar code can be used to generate spatial correlation (instead of covariance) image plots.

Semivariogram Analysis

From now on, in order to simplify computations, we will use a subset of the data containing only observations in July. Computing the empirical semivariogram is much faster when using objects of class `STFDF` rather than `STIDF` since the regular space-time structure can be exploited. We hence take `STObj3` computed in Lab 2.1 (load using `data(STObj3)`) and subset the month of July 1993 as follows.

```
data("STObj3", package = "STRbook")
STObj4 <- STObj3[, "1993-07-01::1993-07-31"]
```

For computing the sample semivariogram we use the function `variogram`.[7] We bin the distances between measurement locations into bins of size 60 km, and consider at most six time lags.

[7]Although the function is named "variogram," it is in fact the sample semivariogram that is computed.

```
vv <- variogram(object = z~1 + lat, # fixed effect component
                data = STObj4,       # July data
                width = 80,          # spatial bin (80 km)
                cutoff = 1000,       # consider pts < 1000 km apart
                tlags = 0.01:6.01)   # 0 days to 6 days
```

The command `plot(vv)` produces Figure 2.17. The plot suggests that there are considerable spatio-temporal correlations in the data; spatio-temporal modeling of the residuals is thus warranted.

Empirical Orthogonal Functions

Empirical orthogonal functions (EOFs) can reveal spatial structure in the data and can also be used for subsequent dimensionality reduction. EOFs can be obtained from the data through either a spectral decomposition of the covariance matrix or a singular value decomposition (SVD) of the detrended space-time data matrix. The data matrix has to be in space-wide format (i.e., where space varies along the columns and time varies along the rows).

For this part of the Lab we use the SST data set. The SST data set does not contain any missing values, which renders our task slightly easier than when data are missing. When data are missing, one typically needs to consider interpolation, median polishing, or other imputation methods to fill in the missing values prior to computing the EOFs.

First we load the sea-land mask, the lon-lat coordinates of the SST grid, and the SST data set itself which is in time-wide format.

```
data("SSTlandmask", package = "STRbook")
data("SSTlonlat", package = "STRbook")
data("SSTdata", package = "STRbook")
```

Since `SSTdata` contains readings over land,[8] we delete these using `SSTlandmask`. Further, in order to consider whole years only, we take the first 396 months (33 years) of the data, containing SST values spanning 1970–2002.

```
delete_rows <- which(SSTlandmask == 1)
SSTdata <- SSTdata[-delete_rows, 1:396]
```

From (2.10) recall that prior to carrying out an SVD, we need to put the data set into space-wide format, mean-correct it, and then standardize it. Since `SSTdata` is in time-wide format, we first transpose it to make it space-wide.

[8] The land SST data are "pseudo-data," and just there to help analysts re-grid the SST data to different resolutions.

```
## Put data into space-wide form
Z <- t(SSTdata)
dim(Z)

## [1]  396 2261
```

Note that Z is of size 396×2261, and it is hence in space-wide format as required. Equation (2.10) is implemented as follows.

```
## First find the matrix we need to subtract:
spat_mean <- apply(SSTdata, 1, mean)
nT <- ncol(SSTdata)

## Then subtract and standardize:
Zspat_detrend <- Z - outer(rep(1, nT), spat_mean)
Zt <- 1/sqrt(nT - 1)*Zspat_detrend
```

Finally, to carry out the SVD we run

```
E <- svd(Zt)
```

The SVD returns a list E containing the matrices $\mathbf{V}$, $\mathbf{U}$, and the singular values $\mathrm{diag}(\mathbf{D})$. The matrix $\mathbf{V}$ contains the EOFs in space-wide format. We change the column names of this matrix, and append the lon-lat coordinates to it as follows.

```
V <- E$v
colnames(E$v) <- paste0("EOF", 1:ncol(SSTdata)) # label columns
EOFs <- cbind(SSTlonlat[-delete_rows, ], E$v)
head(EOFs[, 1:6])

##    lon lat         EOF1         EOF2        EOF3         EOF4
## 16 154 -29 -0.004915064 -0.012129566 -0.02882162 8.540892e-05
## 17 156 -29 -0.001412275 -0.002276177 -0.02552841 6.726077e-03
## 18 158 -29  0.000245909  0.002298082 -0.01933020 8.591251e-03
## 19 160 -29  0.001454972  0.002303585 -0.01905901 1.025538e-02
## 20 162 -29  0.002265778  0.001643138 -0.02251571 1.125295e-02
## 21 164 -29  0.003598762  0.003910823 -0.02311128 1.002285e-02
```

The matrix $\mathbf{U}$ returned from **svd** contains the principal component time series in wide-table format (i.e., each column corresponds to a time series associated with an EOF). Here we use the function **gather** in the package **tidyr** that reverses the operation **spread**. That is, the function takes a spatio-temporal data set in wide-table format and puts it into long-table format. We instruct the function to gather every column except the column denoting time, and we assign the key–value pair EOF-PC:

```
TS <- data.frame(E$u) %>%           # convert U to data frame
      mutate(t = 1:nrow(E$u)) %>%   # add a time field
      gather(EOF, PC, -t)           # put columns (except time)
                                    # into long-table format with
                                    # EOF-PC as key-value pair
```

Finally, the normalized time series are given by:

```
TS$nPC <- TS$PC * sqrt(nT-1)
```

We now can use the visualization tools discussed earlier to visualize the EOFs and the (normalized) principal component time series during July 2003. In Figures 2.20 and 2.21, we show the first three EOFs and the first three principal component time series. We can use the following code to illustrate the first EOF:

```
ggplot(EOFs) + geom_tile(aes(x = lon, y = lat, fill = EOF1)) +
    fill_scale(name = "degC") + theme_bw() +
    xlab("Longitude (deg)") + ylab("Latitude (deg)")
```

Plotting of other EOFs and principal component time series is left as an excercise to the reader. The EOFs reveal interesting spatial structure in the residuals. The second EOF is a west–east gradient, while the third EOF again reveals a temporally dependent north–south gradient. This north–south gradient has a lower effect in the initial part of the time series, and a higher effect towards the end.

EOFs can also be constructed by using `eof` in the package **spacetime**. With the latter, one must cast the data into an `STFDF` object using the function `stConstruct` before calling the function `eof`. The last example in the help file of `stConstruct` shows how one can do this from a space-wide matrix. The function `eof` uses `prcomp` (short for principal component analysis) to find the EOFs, which in turn uses `svd`.

Spatio-Temporal Canonical Correlation Analysis

We can carry out a canonical correlation analysis (CCA) using the package **CCA** in `R`. One cannot implement CCA on the raw data since $T < n$. Instead we carry out CCA on the SST projected onto EOF space, specifically the first 10 EOFs which explain just over 74% of the variance of the signal (you can show this from the singular values in the object `E`). In this example we consider the problem of long-lead prediction, and we check whether SST is a useful predictor for SST in 7 months' time. To this end, we split the data set into two parts, one containing SST and another containing SST lagged by 7 months.

```
nEOF <- 10
EOFset1 <- E$u[1:(nT-7), 1:nEOF] * sqrt(nT - 1)
EOFset2 <- E$u[8:nT, 1:nEOF] * sqrt(nT - 1)
```

The CCA is carried out by running the function **cancor**.

```
cc <- cancor(EOFset1, EOFset2)   # compute CCA
options(digits = 3)              # print to three d.p.
print(cc$cor[1:5])               # print

## [1] 0.843 0.758 0.649 0.584 0.463

print(cc$cor[6:10])

## [1] 0.4137 0.3067 0.2058 0.0700 0.0273
```

The returned quantity `cc$cor` provides the correlations between the canonical variates of the unshifted and shifted SSTs in EOF space. The correlations decrease, as expected, but the first two canonical variates are highly correlated. The time series of the first canonical variables can be found by multiplying the EOF weights with the computed coefficients as follows (see (2.13) and (2.14)).

```
CCA_df <- data.frame(t = 1:(nT - 7),
                     CCAvar1 = (EOFset1 %*% cc$xcoef[,1])[,1],
                     CCAvar2 = (EOFset2 %*% cc$ycoef[,1])[,1])
```

A plot can be made using standard **ggplot2** commands.

```
t_breaks <- seq(1, nT, by = 60)      # breaks for x-labels
year_breaks <- seq(1970,2002,by=5)   # labels for x-axis
g <- ggplot(CCA_df) +
     geom_line(aes(t, CCAvar1), col = "dark blue") +
     geom_line(aes(t, CCAvar2), col = "dark red") +
     scale_x_continuous(breaks = t_breaks, labels = year_breaks) +
     ylab("CCA variables") + xlab("Year") + theme_bw()
```

The plot of the time series of the first canonical variables is shown in Figure 2.23. The plot shows a high correlation between the first pair of canonical variables. What are these canonical variables? They are simply a linear combination of the EOFs, where the linear weights are given in `cc$xcoef[,1]` and `cc$ycoef[,1]`, respectively.

```
EOFs_CCA <- EOFs[,1:4] # first two columns are lon-lat
EOFs_CCA[,3] <- c(as.matrix(EOFs[,3:12]) %*% cc$xcoef[,1])
EOFs_CCA[,4] <- c(as.matrix(EOFs[,3:12]) %*% cc$ycoef[,1])
```

Plotting of the weights as spatial maps is straightforward and left as an exercise. We plot weights (recall these are just linear combination of EOFs) for the lagged SSTs and the unlagged SSTs in Figure 2.24.